(12) INTERNATIONAL APPLICATION PUBLISHED UNDER THE PATENT COOPERATION TREATY (PCT)

(19) World Intellectual Property Organization
International Bureau

(43) International Publication Date
25 March 2010 (25.03.2010)

PCT

(10) International Publication Number
WO 2010/033861 A1

(51) International Patent Classification:
A61K 49/00 (2006.01) *C12Q 1/00* (2006.01)

(21) International Application Number:
PCT/US2009/057569

(22) International Filing Date:
18 September 2009 (18.09.2009)

(25) Filing Language: English

(26) Publication Language: English

(30) Priority Data:
61/098,206 18 September 2008 (18.09.2008) US

(71) Applicants *(for all designated States except US)*: **CEDARS-SINAI MEDICAL CENTER** [US/US]; 8700 Beverly Boulevard, Los Angeles, California 90048 (US). **YEDA RESEARCH AND DEVELOPMENT, CO., LTD.** [IL/IL]; Weismann Institute of Science, P.O. Box 95, 76100 Rehovot (IL). **KORONYO, Yosef** [IL/US]; 453 Alandele Ave., Los Angeles, California 90036 (US).

(72) Inventors; and

(75) Inventors/Applicants *(for US only)*: **KORONYO, Maya** [IL/US]; 453 Alandele Ave., Los Angeles, California 90036 (US). **BLACK, Keith, L.** [US/US]; 1233 Roberto Lane, Los Angeles, California 90077 (US). **SCHWARTZ, Michal** [IL/US]; Department of Neurobiology, Weizmann Institute of Science, Rehovot 76100 (US). **FARKAS, Daniel, L.** [US/US]; 8591 Skyline Drive, Los Angeles, California 90046 (US).

(74) Agents: **AVAKIAN, Patrick** et al.; Davis Wright Tremaine LLP, 865 South Figueroa Street, Suite 2400, Los Angeles, CA 90017 (US).

(81) Designated States *(unless otherwise indicated, for every kind of national protection available)*: AE, AG, AL, AM, AO, AT, AU, AZ, BA, BB, BG, BH, BR, BW, BY, BZ, CA, CH, CL, CN, CO, CR, CU, CZ, DE, DK, DM, DO, DZ, EC, EE, EG, ES, FI, GB, GD, GE, GH, GM, GT, HN, HR, HU, ID, IL, IN, IS, JP, KE, KG, KM, KN, KP, KR, KZ, LA, LC, LK, LR, LS, LT, LU, LY, MA, MD, ME, MG, MK, MN, MW, MX, MY, MZ, NA, NG, NI, NO, NZ, OM, PE, PG, PH, PL, PT, RO, RS, RU, SC, SD,

[Continued on next page]

(54) Title: OPTICAL METHOD FOR THE DETECTION OF ALZHEIMER'S DISEASE

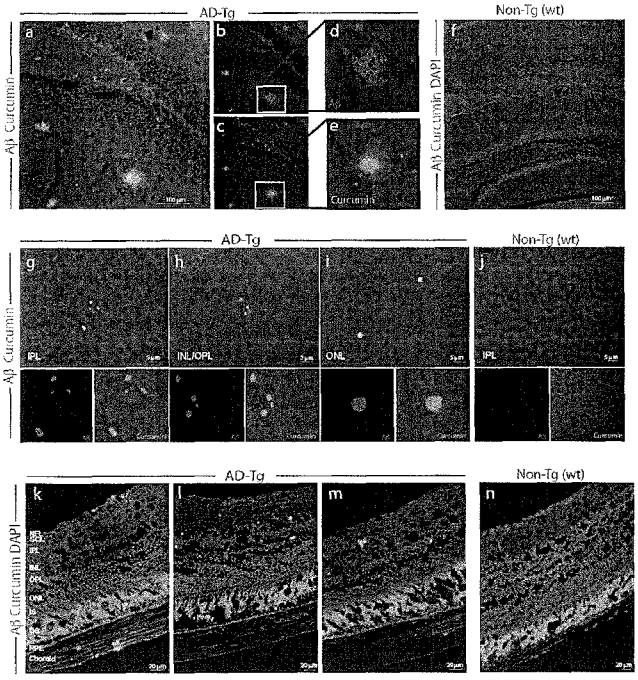

Figure 1

(57) Abstract: The present subject matter relates to a non-invasive optical imaging method for monitoring early pathological events specific to Alzheimer's disease (AD), such as the development, amount and location of amyloid plaques. The ability to monitor such events provides a basis for, among other things, AD diagnosis, prognosis and assessment of potential therapies. In addition, the present subject matter introduces novel methods for treating AD and retinal ailments associated with AD. Aβ-plaque detection in living brains is extremely limited, especially at high resolution; therefore the present invention is based on studies focusing on the eyes as an alternative to brain-derived tissue that can be imaged directly, repetitively and non-invasively.

WO 2010/033861 A1

SE, SG, SK, SL, SM, ST, SV, SY, TJ, TM, TN, TR, TT, TZ, UA, UG, US, UZ, VC, VN, ZA, ZM, ZW.

(84) **Designated States** *(unless otherwise indicated, for every kind of regional protection available)*: ARIPO (BW, GH, GM, KE, LS, MW, MZ, NA, SD, SL, SZ, TZ, UG, ZM, ZW), Eurasian (AM, AZ, BY, KG, KZ, MD, RU, TJ, TM), European (AT, BE, BG, CH, CY, CZ, DE, DK, EE, ES, FI, FR, GB, GR, HR, HU, IE, IS, IT, LT, LU, LV, MC, MK, MT, NL, NO, PL, PT, RO, SE, SI, SK, SM, TR), OAPI (BF, BJ, CF, CG, CI, CM, GA, GN, GQ, GW, ML, MR, NE, SN, TD, TG).

Published:

— *with international search report (Art. 21(3))*

OPTICAL METHOD FOR THE DETECTION OF ALZHEIMER'S DISEASE

FIELD OF THE SUBJECT MATTER

The present subject matter relates to methods for noninvasive monitoring of early pathological events specific to Alzheimer's disease, and thus includes methods and systems for the diagnosis, treatment, prognosis and evaluation of response to treatment of AD.

BACKGROUND OF THE SUBJECT MATTER

All publications herein are incorporated by reference to the same extent as if each individual publication or patent application was specifically and individually indicated to be incorporated by reference. The following description includes information that may be useful in understanding the present invention. It is not an admission that any of the information provided herein is prior art or relevant to the presently claimed invention, or that any publication specifically or implicitly referenced is prior art.

Alzheimer's disease (AD) is a common and devastating age-dependent neurodegenerative disease. AD brain pathology is characterized by typical accumulation of proteolytic products of the amyloid precursor protein (APP), amyloid-β peptides (Aβ), which form extracellular aggregates termed Aβ plaques. These plaques are believed to contribute to disrupted cellular activities and communication in the brain, leading to neurotoxic inflammation and neuronal death [2,3]. Molecular imaging, which allows a non-invasive monitoring of pathological processes in living subjects, has the potential to enhance detection and understanding of disease and drug effectiveness. Accordingly, major efforts have been invested in developing tools to enable noninvasive detection of amyloid plaques through the skull of living AD patients and animal models [4-9]; however, noninvasive monitoring of amyloid plaques is still clinically challenging and of limited availability at high resolution [10-12]. Optical imaging constitutes a powerful, high-resolution and specific tool for in vivo imaging, as recently demonstrated using multiphoton microscopy to image Aβ plaques in vivo in the mouse brain via a cranial window [13]. The present subject matter poses an alternative and noninvasive approach in humans to image the retina of AD patients by optical modalities, provided that Aβ plaques develop in these patients' retinas and share similar properties with those in the brain.

APP is widely expressed in the retinal ganglion cells (RGCs), an outgrowth of the central nervous system (CNS), and is transported to the axonal plasma membrane and the nerve terminals via the optic nerve [14]. Formation of plaques in the retina came recently under investigation, especially in two related neurodegenerative disorders: aged-related macular degeneration (AMD) and glaucoma [50 – 53]. It was unclear whether Aβ-plaques are found in the retina in early or late stage of AD patients. Past evidence pointed to the presence of Aβ-plaques in retinas of glaucoma and AMD patients and their rodent models. For example, Aβ deposition in the RGC layer has been reported in glaucoma patients [50, 51]. In experimental models of glaucoma, apoptosis of RGCs has been associated with the accumulation of Aβ-peptides, and agents targeting their formation were shown to exert neuroprotective activity [52]. In AMD patients, Aβ deposits were found in drusen that correlated with the location of degenerating photoreceptors and retinal pigment epithelium cells [53].

In a Drosophila transgenic model of AD, based on the targeted expression of mutated human APP and presenilin (PS) genes, Aβ immunoreactivity was found in the compound eye, and in association with retinal photoreceptor degeneration [15]. A recent study demonstrated Aβ deposits in the retinal nerve fiber layer (NFL) and ganglion cell layer (GCL) in AD transgenic mice at an advanced stage of the disease (later than 10 months of age). The Aβ deposits were further correlated with neurodegeneration of the RGCs and with microglial activation [16].

Despite this encouraging research, there remains a need in the art for systems and methods for the diagnosis, prognosis and treatment of AD. The present subject matter meets these needs by discovering the presence of Aβ plaques in retinas of postmortem eyes of AD patients. Using mice expressing mutated forms of the human APP and PS1 genes (APPswe/PS1dE9, referred to here as AD-Tg mice), the present subject matter also provides evidence disclosing the early formation of Aβ plaques in the retina prior to their manifestation in the brain. Furthermore, the present subject matter identifies an immune-based therapy, using a weak agonist of a myelin-derived peptide loaded on dendritic cells [17, 18], effective in reducing Aβ plaques in the mouse brains and retinas of AD-Tg mice. Finally, the subject matter demonstrated that systemic injection of curcumin (diferuloylmethane), a natural compound that binds and labels Aβ plaques [19, 20], into live animals allows for non-invasive high-resolution and specific visualization of Aβ plaques in the retina. The present subject matter teaches methods that, for the first time, allow for Aβ

plaques to be detected by number and location, and be repeatedly counted and monitored in real-time in the retina of AD mammals.

BRIEF DESCRIPTION OF THE FIGURES

Exemplary embodiments are illustrated in referenced figures. It is intended that the embodiments and figures disclosed herein are considered illustrative rather than restrictive.

Figure 1 depicts retinal Aβ deposition in the retina of AD-Tg mice visualized by curcumin. Figures 1a - 1f depict images of brain cryosections from 9-month-old AD-Tg (Figures 1a – 1e) and non-Tg (wt) (Figure 1f) mice stained with anti-human Aβ antibody and curcumin *ex vivo*, indicating co-localization of Aβ plaque staining by both detection methods. Figures 1d and 1e depict higher magnification images of plaque staining pattern presented for each channel Figure 1f shows no evidence for double-positive anti-human Aβplaques and curcumin in the non-Tg (wt) mouse. Cell nuclei were labeled with DAPI (blue). Scale bar = 100 μm. Figures 1g - 1j are representative images of retinal whole-mounts from 10-month-old AD-Tg (n=27) and non-Tg (wt) mice (n=18) stained with anti-Aβ antibody and curcumin *ex vivo*. The formation of Aβ plaques (yellow spots of overlapping red and green channels) is demonstrated in several different retinal layers: Figure 1g depicts IPL-Inner Plexiform Layer, Figure 1h depicts INL-Inner Nuclear/OPL-Outer Plexiform Layers, and Figure 1i depicts ONL-Outer Nuclear Layer. Figure 1J shows Aβ plaques were essentially absent in the non-Tg (wt) mice. (Figure 1g and 1j, lower row). Higher magnification images for separate channels demonstrate plaque-staining patterns with both procedures. Scale bars = 5 μm. Figures 1k - 1n depicts whole eye sagittal cryosections stained with curcumin *in vivo*, followed by anti-human Aβ antibody and DAPI *ex vivo*. In Figures 1k - 1m, Aβ plaques were detected in most retinal layers and in the choroid in 10-month-old AD-Tg mice. In Figure 1n Aβ plaques were undetectable in the retina and choroid of non-Tg (wt) mice. Scale bar = 20 μm.

Figure 2 depicts Aβ plaques in the human retina of Alzheimer's disease patients. Figures 2a and 2b are representative images of the human whole-mount retina of an 87-yr-old AD patient after staining with Sudan Black B to eliminate non-specific autofluorescence signals, and following curcumin *ex vivo* staining (curcumin-labeled plaques are indicated by white arrows). Scale bars = 10 μm. Cell nuclei are labeled with DAPI (blue). Figures 2c and 2d show higher magnification images of the human whole-mount retina of an 65-yr-old AD patient following Sudan Black B staining (black spots for Sudan staining), and then

curcumin staining (curcumin-labeled plaque is indicated by white arrow). Scale bars = 5 μm. Figures 2e - 2g provide additional examples of curcumin-positive plaques in retinas of a series of 65- to 90-yr-old human AD patients. Figures 2h - 2j are representative images of human whole-mount retinas of 65- and 87-yr-old human AD patients stained with anti-human Aβ antibodies followed by Sudan Black B treatment at several retinal depths (to include RGC and IPL). Figure 2i represents a higher magnification image of the retinal plaque. Aβ plaque morphology was similar to that found in the mouse retinas and brains. Scale bars = 5 μm. Figures 2k - 2m represent subsequent staining of the same human retinas with curcumin, which reveals that the plaques were selectively colabeled with human Aβ antibodies and curcumin (lower row images for separate channels). Figure 2n depicts double staining with human Aβ antibodies and curcumin in postmortem non-AD human retinal whole mount showing no signs of Aβ plaques (lower row images for separate channels). Scale bars = 5 μm.

Figure 3 depicts mouse retinal Aβ plaque formations at the pre-symptomatic early stage and accumulation during disease progression. Following i.v. curcumin injections into the tail vein, Aβ plaques were visible in AD-Tg mice retinas and brains. Figures 3a - 3n are representative z-axis projection images of whole-mount retinas from AD-Tg (n=18) and non-Tg (wt; n=10) mice at various ages; Figures 3a - 3d depict 2.5-month-old AD-Tg mouse, with Figure 3a showing presence of plaques in the retina and Figure 3b showing validation of Aβ plaque staining using specific anti-human antibody *ex vivo* at the same location (co-localization of curcumin and Aβ antibody in yellow). Scale bars =10 μm. Figures 3c and 3d show no plaques were detected in the brain hippocampus and cortex. Scale bars = 100 μm. Figures 3e - 3h depict 5-month-old AD-Tg mouse, with Figure 3e depicting the presence of plaques in the retina and Figure 3f following specific Aβ antibody staining *ex vivo*. Scale bars =10 μm. Figures 3g and 3h show detection of plaques in the brain. Scale bars = 50 μm. Figures 3i - 3k depicts 9-month-old AD-Tg mouse, with Figure 3i showing multiple plaques in the retina and Figures 3j and 3k showing plaques in the brain. Scale bars (i) = 10 μm and (j,k) = 50 μm. Figures 3l - 3n depict 17-month-old AD-Tg mouse, with Figure 3l showing numerous plaques in the retina and Figures 3m and 3n showing plaques in the brain. Scale bars (i) = 10 μm and (m,n) =100 μm. Figures 3o - 3q depicts 9-month-old non-Tg (wt) mouse, with Figure 3o showing no plaques in the retina and Figures 3p and 3q showing no plaques in the brain. Scale bars (o) = 10 μm and (p,q) =100 μm.

Figure 4 depicts decreased Aβ plaques in the retina of AD-Tg mice following dendritic cell-based vaccination. Figures 4a - 4g are representative z-axis projection images of whole-mount retinas from 10 month-old mice, Figures 4a - 4c show PBS-treated AD-Tg mouse control, Figures 4d - 4f show vaccinated AD-Tg mouse, and Figure 4g shows non-Tg (wt) mouse stained *ex vivo* with curcumin and anti-human Aβ antibodies. Figures 4b and 4c, and Figures 4e and 4f depict separate channel images for curcumin and anti-Aβ antibodies labeling in the retina. Scale bars = 10 μm. Figure 4h is an illustration of 12 regions around the optic disc (indicated by rectangles 1-12) representing the area covered for quantitative analyses of plaques in the retinal whole-mounts (n=4 mice per group; two retinas per mouse). Scale bar = 200 μm. Figure 4i depicts the decrease in plaque number, observed in the retinas of AD-Tg mice treated with immunebased vaccination as compared to PBS-treated controls (*Student's t-test; P=0.0028*). Figure 4j depicts a decrease in mean plaque area, observed in the retinas of vaccinated AD-Tg mice as compared to their controls (*Student's t-test P=0.0002*). Figure 4k shows that the significant reduction in the total area covered by plaques was also detected in the brain hippocampus and cortex of the same mice following immune-based vaccination (*Student's t-test P=0.0085*). Error bars in each panel represent SEM.

Figure 5 depicts *in vivo* imaging of curcumin-labeled plaques in AD-Tg mouse retinas. Figure 5a - 5c are representative z-axis projection images taken from retinal whole-mounts of non-perfused AD-Tg versus non-Tg (wt) mice (10-month-old), following i.v. curcumin or PBS administration *in vivo* (blood vessels are indicated by red arrows). Figure 5a shows Aβ plaques were visible (indicated by white arrows) in AD-Tg mouse retinas following i.v. injection of curcumin (n=6). Figure 5b shows plaques were undetectable in the retinas of AD-Tg mice after i.v. injection of PBS (n=5). Figure 5c shows plaques were undetectable in the retinas of non-Tg (wt) mice following i.v. injection of curcumin (n=5). Figure 5d is a representative confocal z-axis projection image, using three channels and sagittal/coronal virtual sections, demonstrating Aβ plaques (plaques inside the vessels indicated with white arrows), stained with anti-human Aβ antibodies, in the parenchyma and inside the blood vessels of AD-Tg mouse retinal whole-mount. Figures 5e and 5f depict images captured using a fluorescence microscope with AOTF-based spectral imaging system, and analyzed and visualized by segmentation and classification software. In Figure 5e, Aβ plaques (in white) and blood vessels (indicated by arrows), were visible in a retinal whole-mount stained *in vivo* with curcumin and imaged at a single channel (ex. 562/40 nm; em.

624/40 nm). Figure 5f depicts a spectrally-classified image using optical signature (OS) specific to Aβ plaques labeled with curcumin in the same retinal whole-mount and region. Aβ plaques are shown in pseudocolor (indicated by white arrows) and all non-plaque tissue is in green pseudocolor. Scale bars = 10 μm. Figures 5g - 5j are images following a single injection of curcumin, wherein plaques (indicated with white arrows) were visible in live AD-Tg mouse retinas (n=4) by emission of light following excitation with a spectrally controlled source (wavelength of 546/15 nm). Figures 5i and 5j are higher magnification images, where plaques were mostly detected in areas close to the optic disc and the average plaque size was compatible with that observed in the whole-mount retinas (*ex vivo*). Figure 5k shows no plaques detected in the non-Tg (wt) mice (n=4) i.v. injected with curcumin. Scale bars (g, k) = 100 μm, and (h-j) = 10 μm. 23.

Figure 6 depicts a flow diagram of a spectral imaging system for diagnosing, prognosing, and analyzing Aβ plaques in accordance with an embodiment of the present invention.

Figure 7 depicts a flow diagram of a spectral imaging system for diagnosing, prognosing and/or analyzing Aβ plaques in accordance with an embodiment of the present invention.

Figure 8 depict high-resolution images of small retinal plaques (mostly <1 μm in diameter), which were found to originate from the endogenous mouse APP gene. Images are of a 10 month old Non-Tg(wt) mouse retina.

Figure 9 depicts images of live AD-Tg and Non-Tg(wt) mouse retinas showing curcumin stained plaques in the AD-Tg retina, and the lack of curcumin stained plaques in the Non-Tg(wt) retina.

DETAILED DESCRIPTION OF THE INVENTION

All references cited herein are incorporated by reference in their entirety as though fully set forth. Unless defined otherwise, technical and scientific terms used herein have the same meaning as commonly understood by one of ordinary skill in the art to which this invention belongs. Singleton *et al.*, *Dictionary of Microbiology and Molecular Biology 3rd ed.*, J. Wiley & Sons (New York, NY 2001); March, *Advanced Organic Chemistry Reactions, Mechanisms and Structure 5th ed.*, J. Wiley & Sons (New York, NY 2001); and Sambrook and Russel, *Molecular Cloning: A Laboratory Manual 3rd ed.*, Cold Spring Harbor

Laboratory Press (Cold Spring Harbor, NY 2001), provide one skilled in the art with a general guide to many of the terms used in the present application.

One skilled in the art will recognize many methods and materials similar or equivalent to those described herein, which could be used in the practice of the present invention. Indeed, the present invention is in no way limited to the methods and materials described.

"Administering" and/or "Administer" as used herein refer to any route for delivering a pharmaceutical composition to a patient. Routes of delivery may include non-invasive peroral (through the mouth), topical (skin), transmucosal (nasal, buccal/sublingual, vaginal, ocular and rectal) and inhalation routes, as well as parenteral routes, and other methods know in the art. Parenteral refers to a route of administration that is generally associated with injection, including intraorbital, infusion, intraarterial, intracarotid, intracapsular, intracardiac, intradermal, intramuscular, intraperitoneal, intrapulmonary, intraspinal, intrasternal, intrathecal, intrauterine, intravenous, subarachnoid, subcapsular, subcutaneous, transmucosal, or transtracheal. Via the parenteral route, the compositions may be in the form of solutions or suspensions for infusion or for injection, or as lyophilized powders.

"Alzheimer's Disease" as used herein refers to all form of dementia, identified as a degenerative and terminal cognitive disorder. The disease may be static, the result of a unique global brain injury, or progressive, resulting in long-term decline in cognitive function due to damage or disease in the body beyond what might be expected from normal aging.

"Age-related macular degeneration" as used herein refers to is a medical condition in older adults that results in a loss of vision in the center of the visual field (the macula) due to damage to the retina.

"Cataracts" as used herein refers to a clouding that develops in the crystalline lens of the eye or in its envelope, varying in degree from slight to complete opacity and obstructing the passage of light. Early in the development of age-related cataract the power of the lens may be increased, causing near-sightedness (myopia), and the gradual yellowing and opacification of the lens may reduce the perception of blue colors. Cataracts typically progress slowly to cause vision loss and are potentially blinding if untreated.

"Fluorescent Marker" as used herein refers to any and all compounds containing flurophore for attaching the compound to another molecule, such as a protein or nucleic acid. This is generally accomplished using a reactive derivative of the fluorophore that selectively binds to a functional group contained in the target molecule.

"Glaucoma" as used herein refers to a group of diseases that affect the optic nerve and involves a loss of retinal ganglion cells in a characteristic pattern. Glaucoma is categorized

as a type of optic neuropathy.

"Mammal" as used herein refers to any member of the class *Mammalia*, including, without limitation, humans and nonhuman primates such as chimpanzees, and other apes and monkey species; farm animals such as cattle, sheep, pigs, goats and horses; domestic mammals such as dogs and cats; laboratory animals including rodents such as mice, rats and guinea pigs, and the like. The term does not denote a particular age or sex. Thus adult and newborn subjects, as well as fetuses, whether male or female, are intended to be including within the scope of this term.

"Therapeutically effective amount" as used herein refers to that amount which is capable of achieving beneficial results in a mammal being treated. A therapeutically effective amount can be determined on an individual basis and can be based, at least in part, on consideration of the physiological characteristics of the mammal, the type of delivery system or therapeutic technique used and the time of administration relative to the progression of the disease, disorder or condition being treated.

"Treat," "treating" and "treatment" as used herein refer to both therapeutic treatment and prophylactic or preventative measures, wherein the object is to prevent or slow down (lessen) the targeted pathologic condition, disease or disorder even if the treatment is ultimately unsuccessful. Those in need of treatment may include those already with the disorder as well as those prone to have the disorder or those in whom the disorder is to be prevented.

β-Amyloid deposition is central to AD neuropathology and a key hallmark of Alzheimer's disease. However, monitoring Aβ plaques in the brains of living Alzheimer's patients and animals is limited by the current resolution and specificity of MRI and PET, and a definite diagnosis of Alzheimer's or other ailment or condition characterized by the formation of Aβ plaques is only possible after brain tissue autopsy by monitoring number and distribution of plaques and tangles. Hence, developing means to identify plaques *in vivo* is essential for diagnosis as well as for evaluation of disease progression in response to therapies.

The present subject matter establishes the formation of retinal Aβ plaques in mammals and teaches a method for identifying, quantizing, and imaging retinal Aβ plaque. The present subject matter may be incorporated for patients with Alzheimer's disease, dementia, and other clinical conditions and ailments characterized by the formation of Aβ

plaques. Furthermore, the present subject matter discovered that the formation of Aβ plaques in the retina of AD patients preceded their appearance in the brain. Accordingly, the present subject matter discloses a method for early diagnosis of AD in a mammal comprising the steps of administering a fluorescent marker to the patient for staining Aβ plaques in the retina, and imaging the retina of the patient with a optical imaging system to identify stained Aβ peptides.

Another embodiment of the present subject matter teaches a method for prognosing AD in mammals by measuring the increase or decrease of Aβ plaques in the retina of patients before and after treatment. The method of prognosis comprises the steps of administering a fluorescent marker to the patient for staining Aβ plaques in the retina and imaging the retina of the patient with an optical imaging system to identify stained Aβ peptides, followed by administering an AD treatment to the patient and allowing due course for the AD treatment to take effect. And, re-administering a fluorescent marker to the patient for staining Aβ plaques in the retina after AD treatment and imaging the retina of the patient with the optical imaging system to identify an increase or decrease in stained Aβ peptides.

In a further embodiment, the present subject matter discloses a method for treating AD in mammalian patients, comprising administering a therapeutically effective amount of myelin-derived peptides and/or agonist of myelin-derived peptides to the patient in reducing the formation of, and dissolving the existence of Aβ plaques.

The present subject matter also finds utility in disclosing methods for improving eyesight in mammalian patients containing retinal Aβ plaques, comprising the steps of administering a therapeutically effective amount of myelin-derived peptides and/or agonist of myelin-derived peptides to the patient. The method of improving eyesight may be applicable for patients with AD, dementia, or other clinical conditions and ailments characterized by the formation of Aβ plaques, such as Age-Related Macular Degeneration (AMD), and glaucoma.

In further embodiments the subject matter describes that Aβ plaques are present in the retina of mammals and may be utilized to analyze, prognose and diagnose a multitude of other clinical conditions and ailments characterized by retinal Aβ plaques. Representative clinical condition and ailments may include AMD and glaucoma.

Further discoveries identified in the present subject matter include an optical imaging system for visualizing Aβ plaques *in vivo* in the retina of non-human mammalian and human patients. The optical imaging system incorporates the use of a fluorescence microscopes, mercury and xenon arc lamps, a CCD camera, an AOTF (acousto-optic tunable filters)-based

spectral image acquisition apparatus, and post-analysis imaging software. The optical imaging system incorporates the foregoing tools to provide retinal images of stained Aβ plaques, providing a visual pseudo-color representation of the spectral signature extracted from the raw images, representing the size and location of the Aβ plaques objects.

In an alternative embodiment, the optical imaging system incorporates the use of a stereomicroscope that is adjusted to visualize fluorescence and scatter signals at higher resolutions. The stereomicroscope may be fitted with a Polychrome V variable wavelength light source. In additional embodiments, the optical imaging system may incorporate a MicroFire color digital camera and one or more magnifying lenses to improve magnification and image detail. Image acquisition is attained and perfected by post-analysis image segmentation and classification using imaging software.

In further embodiments, the optical imaging system may be incorporated in methods for diagnosing, prognosing, and treating Aβ plaques in mammals. Furthermore, the optical imaging system may be augmented with adaptive optics, used to improve the performance of the optical imaging system by reducing the effects of rapidly changing optical distortion.

In yet another embodiment, the subject matter method may be utilized for drug development and testing. As the non-invasive, rapidly repetitive imaging methods would enable back-to-back comparison of various drugs and various dosage of drugs, the present subject matter would find favorable utility in drug development and testing.

A previous report has identified Aβ pathology in the brain, based on the finding of Aβ accumulation in the lenses of AD patients [31]. The current study provides evidence for the existence of Aβ plaques in the retinas of AD patients that could be specifically visualized by curcumin. Aβ plaques were found in the retina of all examined AD patients, whereas they could not be detected in the non-AD controls. In both young as well as in aged AD mice, a good correlation between retinal and brain Aβ plaque pathology was observed; plaques accumulated in an age-dependent manner during disease progression, and both retina and brain showed Aβ plaque reduction as a response to the same therapeutic modality. Overall, the retinal tissue, which shares many similarities with the brain, can potentially be used for diagnosis and monitoring of AD.

In the present study, Aβ plaques in the retinas of the AD patients were detected mostly within the RGC layer. In AD mouse eyes, plaques were seen in most of the retinal layers and in the choroid. Plaques were noticeable from the NFL to the ONL, and clusters of Aβ plaques were seen more often in the inner layers of the retina, signifying the possibility of

plaque imaging through the eyes of living subjects. Retinas of AD mice undergo an age-dependent increase in Aβ plaque load in terms of both number and size, similar to the age-dependent accumulation of plaques observed in the brain. Our results demonstrating retinal plaque pathology are consistent with a recent report that reveals retinal Aβ deposition in correlation with retinal inflammation and degeneration in adult and aged AD-Tg mice [16]. The present subject matter, we not only provides evidence supporting a link between retinal and brain plaque pathology, but also show that Aβ plaques are detectable in the retina prior to their detection in the brain, in young AD-Tg mice. We were further able to show a significant reduction of Aβ plaques in the retinas of AD-Tg mice following vaccination with myelin-derived peptide; this treatment as well as related ones were found to be effective in attenuating Aβ plaque burden in the brain [17,24,25]. These findings provide that assessment of retinal plaques may be used to evaluate responses to plaque-reducing therapy, and that retinal plaques may respond to the same treatment that is effective in Aβ plaque reduction in the brain.

Importantly, the fact that plaques were seen in the GCL in the human eyes, reaching a size of more than 5 μm, makes imaging Alzheimer's patients through the retina a feasible approach, with some modifications, even with the currently available tools for human eye imaging, such as an adaptive optics ophthalmoscope [32]. In live mice, a commercially available mydriatic retinal camera, was found to be effective in recording fundus photographs enabling evaluation of longitudinal changes of retinal ganglion cells [33]. A blue-light confocal scanning laser ophthalmoscope (bCSLO) system that was modified to visualize cyan fluorescent protein, also provides a noninvasive approach to visualize RGCs in the living mouse retina [34]. Here, for the proof-of-concept, we were able to detect curcumin-labeled plaques in live mice using a stereomicroscope (Leica S6E) equipped with Polychrome V spectral light source and double convex lens. Moreover, using an AOTF system, we were able to detect retinal Aβ plaques by curcumin while eliminating strong background autofluorescence signals (from red blood cells).

In the present study, curcumin was effective in detecting retinal Aβ plaques when systemically administered at a single dose of 7.5 mg/kg or when given orally. Curcumin demonstrated the ability to cross the blood-brain and blood-retina barriers, which is a requirement for a useful plaque-imaging agent. In terms of safety, Phase I and II trials using curcumin in patients with cancer have proven its low toxicity in humans even at high doses (12 g/day), and when given over extended periods of time [35]. Translation of curcumin doses given intravenously or orally, from mice to humans (below 1 g) for retinal plaque

visualization, is expected to remain within the reported safety levels. Furthermore, recent studies have reported various approaches to significantly increase curcumin stability and bioavailability in humans [36].

The identification of Aβ plaques in the retina of AD patients, provides a novel opportunity for developing a high resolution and sensitive imaging method, that will allow their detection *in vivo*. These results may be consistent with the early visual dysfunctions found in AD patients [37,38], and with the evidence for retinal abnormalities such as loss of cells in the GCL and atrophy of the NFL, reported in AD patients [39-44]. Although it is unclear whether Aβ plaques are found in the retina at early or later stages of AD, the current discovery of Aβ plaques in the retina of these patients at different ages, and the fact that these plaques are detectable at a very early pre-symptomatic phase of the disease in AD-Tg mice, strengthens the possibility that curcumin-labeled plaques, seen through the eyes, could be used for early diagnosis of AD. Importantly, based on their unique size and distribution within the retinas, the plaques observed in AD patients could be eventually used for differential diagnosis: plaques that were detected in age-related macular degeneration are locally restricted to retinal pigment epithelium within drusen and appear smaller in size [45-47]. In terms of the retinal abnormalities seen in AD patients, it is possible that a plaque-reducing therapy, such as the current DC vaccination, may also help to ameliorate some of the visual dysfunctions, even leading to improved eyesight.

Along with aging of the world's population and the growing epidemic of AD, an early detection of AD becomes ever more critical for evaluating risk, assessing new therapies, and treating AD with early intervention once it has developed. AD pathology, including amyloid plaques and neurofibrillary tangles, is believed to appear many years before symptoms manifest and before any substantial neurodegeneration occurs. Discovery of early measurable markers specific to AD, such as the Aβ-plaques in the retina, which may predict development of brain pathology and cognitive decline in still cognitively normal subjects, is especially needed. The inventors' findings in mice models of AD support the use of imaging of retinal plaques *in vivo* labeled with curcumin as a non-invasive tool for early indication of AD pathology and response to a therapeutic intervention.

Furthermore, the present subject matter introduces vaccination therapies to reduce and/or eliminate Aβ-plaques in the retina, often associated with degeneration of the eyes and eyesight in AD patients. Myelin-derived peptides or weak agonists of myelin-derived

peptides were used to effectively induce neuroprotection and to reduce plaque formation in the retina.

In summary, we identified Aβ plaques in human retinas, and describe a new approach to detect and monitor Alzheimer's plaque pathology earlier and more readily than in the brain, by imaging Aβ plaques in the retina using a systemically administered compound, proven safe in humans. This may predict development of brain pathology and cognitive decline in subjects who are still cognitively normal and well before a significant functional deficit is seen. These findings show that optical imaging of the retina can be used as a noninvasive approach for monitoring AD progression and response to therapeutic interventions [48].

EXAMPLES

The following examples are provided to better illustrate the claimed invention and are not to be interpreted as limiting the scope of the invention. To the extent that specific materials are mentioned, it is merely for purposes of illustration and is not intended to limit the invention. One skilled in the art may develop equivalent means or reactants without the exercise of inventive capacity and without departing from the scope of the invention.

Example 1

Results

Aβ deposits in AD mouse retina can be visualized using curcumin

AD-Tg mice carrying the human APPswe and PS1dE9 transgenes were used to assess the potential of developing a noninvasive tool for detecting Aβ plaques in the eye. We first verified that curcumin had an affinity to the same plaques that were detected by antibodies specific to human Aβ in the hippocampus of AD-Tg mice (Figure 1a; separate channels Figures 1b and 1c). At higher magnification, images show the specific staining pattern obtained following each procedure (Figures 1d and 1e). Human Aβ-plaques were undetectable in the brains of non-Tg littermate wild type (wt) mice (Figure 1f). We then tested whether Aβ plaques in the eyes of AD-Tg mice could also bind curcumin. Examination at high resolution revealed the presence of Aβ plaques labeled by both curcumin and anti-human Aβ-antibodies in the retinas of AD-Tg mice (Figure 1g - 1i, retinal whole mount; Figure 1k - 1m, cross-section) but not in the retinas of non-Tg (wt) mice (Figure 1j and 1n). The representative images display the location of Aβ plaques in retinal whole

mounts at various depths (consecutive acquisition at focal planes of 80 μm depth) to include the inner plexiform layer (IPL; Figure 1g), inner nuclear layer (INL) / outer plexiform layer (OPL; Figure 1h), and outer nuclear layer (ONL; Figure 1i). Analysis of cross sections further verified Aβ plaque deposition in deep retinal layers and the choroid, with an apparent predominance in the ganglion cell layer (GCL) and IPL through OPL layers (Figure 1k - 1m). Whereas human-Aβ plaques were absent in the non-Tg (wt) littermates (Figure 1j and 1n), occasional small curcumin-positive plaques were detected. To determine the nature of these small and sparse plaques that were detected by curcumin staining in wt mice, we carried out a double-staining experiment using curcumin and antibodies specific to mouse-Aβ in wholemount retinas of 10-month old wt mice. Indeed, the small plaques detected by curcumin in the wt retinas were found to be co-labeled with the anti-mouse Aβ antibodies, thus confirming their identity as endogenously formed mouse-Aβ deposits (Figures 8a - 8d).

Example 2

Results

Aβ plaques are formed in retinas of AD patients and could be visualized by curcumin

We next examined the presence of Aβ plaques in postmortem eyes of patients with definite diagnosis of AD (n=9; age range from 48 to 94 years; different disease severities, categorized based on their neuropathology reports), and in postmortem eyes of age-matched normal controls (n=4; 66 to 92 years; see human donor eye records in (see Table 1). Autofluorescence and non-specific signals of fixed human eyes observed under excitation ranging from 360-710 nm and associated with lipofuscin/lipid deposits and/or long-term fixation with formalin [21, 22], were eliminated by Sudan Black B staining (Figure 2). For curcumin staining, we first immersed human whole-mount retinas with Sudan Black B (Figure 2a and 2c; no plaques were observed), followed by exposure to curcumin (Figure 2b and 2d; representative images display plaques within the same tissue location). Plaques detected by curcumin, ranging in size from 1 to 10 μm (typically around 5 μm), were found in all AD patient eyes examined, at various focal depths corresponding to the GCL, IPL and INL retinal layers (Figure 2a and 2g), and with an apparent correlation to the reported plaque pathology in the brain. We also analyzed the human retinas with antibodies directed against human Aβ. We identified Aβ plaques in AD patients and found that their structure was similar to that found in the mouse retina and brain [Figures 2h and 2i represent the innermost retinal layers (i.e. GCL) where the plaques are easily detected; Figure 2i is a higher magnification image of the retinal Aβ plaque structure; Figure 2j represents deeper

consecutive focal planes (i.e. IPL)]. The plaques could not be detected when only secondary antibodies were used (data not shown). Exposure of the human retinas to curcumin after their immunolabeling for Aβ, confirmed their co-localization (Figure 2k - 2m). In non-AD human eyes, no Aβ plaques were detected (Figure 2n).

TABLE 1

Patient #	Gender[1] & Age (yrs)	Pre-Mortem Diagnosis (Disease Duration)	Post-Mortem Neuropathology	Final Diagnosis	Cause Of Death
412	F, 48	Dementia, AD (10 yrs)	Moderate to frequent NPs and NFTs in the neocortex and hippocampus	AD definite	Cerebral atrophy with hydrocephalus
404	F, 65	Dementia, AD (5 yrs)	Large no. of diffuse plaques. NPs, NFTs in the entorhinal cortex and hippocampus	AD definite	N/A
435	M, 70	Dementia, AD (5 yrs)	Moderate no. of NPs and NFTs	AD definite	Pneumonia of posterior lungs
539	M, 78	Dementia (3 yrs)	Large no. of NPs most with cores and abundant NFTs and diffuse plaques	AD definite	Subdural hematoma
484	M, 86	Dementia, AD (11yrs)	Abundant NFTs and NPs in the neocortex and hippocampus	AD definite	Cerebrum & Cerebellum infarction
664	M, 87	Dementia, AD (8 yrs)	Moderate to frequent NPs with NFTs in the neocortex and Hippocampus CA-1	AD definite	Cerebrum infarction
486	F, 88	Dementia, AD (6 yrs)	Severe NPs and NFTs	AD definite	Pneumonia
513	F, 90	Dementia, AD[2] (14 yrs)	Mild NPs[3] and abundant NFTs[4]	AD definite[6]	Cerebral hemorrhage infarction focal
525	F, 94	Dementia, AD (11 yrs)	Abundant NPs with mature cores and numerous NFTs	AD definite	Cerebrum infarction
93-78	M, 66	Absence of Dementia Normal	N/A	Normal Brain	Liver failure
93-111	M, 77	Absence of Dementia Normal	N/A	Normal Brain	Sepsis
476	M, 88	Absence of Dementia Occipital CVA[5]	Sparse neocortical NPs and NFTs	Normal Brain	Cerebrum infarctions
529	F, 92	Absence of Dementia Normal	Moderate no. of diffuse plaques and small no. of NPs only in the hippocampus	Normal Brain	Cerebrum infarction remote multiple

[1] Gender: F=Female. M=Male
[2] AD - Alzheimer's disease
[3]Neuritic Plaques (NPs) and [4]Neurofibrillary Tangeles (NFTs) were determined by Silver (Gallyas or Bielschowsky) stain and Thioflavin stain in several CNS Sites: Hippocampus CA-1. Entorhinal Cortex. Mid Frontal. Sup./Mid. Temporal. Inferior parietal. Primary Visual. Visual association area.
[5] CVA – Cerebral vascular accident or stroke.
[6] AD definite – According to CERAD criteria.

Example 3

Results

Aβ plaques in AD mice, stained in vivo by curcumin, are detected in the retina earlier than in the brain and accumulate during disease progression

To establish the use of curcumin for imaging plaques in the retina, we tested its bioavailability to the eye when injected systemically. To this end, mice were intravenously injected with curcumin. Labeled plaques following the administered curcumin could be detected in the retinas and brains of AD-Tg mice, but not in the non-Tg (wt) controls (Figure 3). These findings confirmed that curcumin crosses the blood-brain barrier and suggest that it also crosses the blood-retina barrier and has a high affinity for Aβ plaques *in vivo*. Importantly, curcumin-labeled plaques could be detected following a single curcumin injection or following multiple injections. Representative z-axis projections of retinal and brain hippocampus and cortical images of AD-Tg mice at the ages of 2.5, 5, 9 and 17 months demonstrated an age-dependent correlation between plaque deposition in the retina and the brain, and increased accumulation over the course of disease progression (Figure 3a - n). Importantly, plaques were detected in the retina (Figure 3a and 3b) but not in the brain (Figure 3c and 3d) as early as at 2.5 months of age in AD-Tg mice following *in vivo* curcumin administration, suggesting that Aβ plaques in the retinas precede brain pathology. We further confirmed that these curcumin-labeled plaques were co-localized *ex vivo* with anti-human Aβ antibody staining (Figure 3b and 3f). Aβ plaques were first detectable in the brain at the age of 5 months (Figure 3g and 3h), in line with previous descriptions of disease initiation and progression in this strain of AD-Tg mice [23]. In the wt mice, Aβ plaques were undetectable both in the retina (Figure 3o) and in the brain (Figure 3p and 3q) as late as 9 months of age.

Example 4

Results

Aβ plaque burden is decreased in the retina following vaccination therapy

We further investigated whether the fate of retinal plaques observed in AD-Tg mice, is similar to that of brain Aβ plaques in response to the same treatment. Myelin-derived peptides or weak agonists of myelin-derived peptides have been shown to effectively induce neuroprotection and to reduce plaque formation [24-26]. To ensure the beneficial effect of the vaccination without the risk of inducing autoimmune encephalomyelitis, we chose to vaccinate AD-Tg mice with an altered myelin-derived peptide (MOG45D, derived from

MOG 35-5527,28) using dendritic cells (DCs) as a carrier and adjuvant. Whole-mounted retinas of 10-month old AD-Tg mice injected with either MOG45D-loaded DCs or with PBS, and those of wt littermates (4 mice/8 retinas per group), were *ex vivo* labeled for Aβ plaques, using both curcumin and anti-Aβ antibody (Figure 4). Representative axial (z-stack) projection images demonstrated substantial reduction of the number of Aβ plaques in vaccinated AD-Tg mice compared to PBS-treated controls (Figure 4a - 4c versus Figure 4d and 4f, respectively; separate channels in Figures 4b and 4c, and Figures 4e and 4f). No Aβ plaques (double stained with curcumin and antihuman Aβ antibody) were detected in the wt mice (Figure 4g). In high-resolution images, we occasionally detected small retinal plaques (mostly <1 μm in diameter), which were found to originate from the endogenous mouse APP gene (Figure 8). These small plaques were stained by curcumin but not by anti-human Aβ antibodies in all three experimental groups (Figures 4a, 4d and4g). We further quantified plaque number and size by capturing 12 areas (total of approx. 0.45 mm2) around the optic disc, and quantified plaques across a 60-μm scanning depth in each area (Figure 4h; each area is indicated by rectangle 1-12). A significant decrease in plaque number detected by curcumin staining was found in the retinas of vaccinated AD-Tg mice compared to PBS-treated controls (Figure 4i; *P=0.0028*). Substantial reduction was also observed in the average area covered by the retinal plaques in vaccinated versus PBS-treated AD-Tg mice (Figure 3j; *P=0.0002*). Notably, significant reduction, relative to PBS-treated mice, in the total plaque area was also observed in the hippocampus and cortex from the brains of the same vaccinated mice (Figure 4k; *P=0.0085*).

Example 5

Results

In vivo imaging of Aβ plaques in the eyes using systemically injected curcumin

To further investigate the potential of visualizing Aβ plaques by curcumin in the eyes of live subjects, we first tested our ability to identify Aβ plaques in whole-mount retinas of mice that were not perfused prior to their eye enucleation, a more physiological setting. Representative axial projection images demonstrated that even under these conditions, which included background signals from red blood cells in the capillaries, plaques could be identified in the retinas of AD-Tg mice that had been previously i.v. injected with curcumin (Figure 5a). Importantly, in the absence of curcumin, plaques were undetectable in AD-Tg mice that had been i.v. injected with PBS (Figure 5b), suggesting that when using these imaging modalities, plaques are barely detectable in the retina solely by their

autofluorescence signals. As expected, in non-Tg(wt) mice injected with curcumin, plaques were also not detected (Figure 5c). Additional labeling of plaques with anti-human Aβ antibodies *ex vivo*, confirmed the Aβ specificity of curcumin staining (data not shown). Aβ plaques in whole-mount retinas of ADTg mice labeled with anti-Aβ antibodies were found inside blood vessels as well as in their parenchymal vicinities (Figure 5d; confocal virtual cross-section). We further assessed whether it would be possible to detect Aβ plaques while reducing the background signal emerging from blood vessels. To this end, we monitored the specific optical signature using a fluorescence microscope (Nikon TE2000) including a multi-spectral imaging technology, comprised of spectral imaging with acousto-optic tunable filters (AOTF) [29] and fluorescence lifetime imaging using a gated camera; image acquisition was followed by post-analysis image segmentation and classification using software that was previously developed by us [30]. Curcumin-labeled plaques imaged using a microscope equipped with AOTF at a single wavelength channel were observed in AD-Tg mouse retina (Figure 5e). By applying the AOTF-based imaging, capturing the spectral signature of curcumin-labeled plaques, and post-translation into color-classified digital images, we were able to identify the specific optical signature of Aβ plaques as "true" signals, while eliminating the autofluorescence noise generated by the blood vessels (Figure 5f). To investigate the feasibility of our approach for noninvasive plaque detection, we conducted an *in vivo* imaging of the retina in live mice using a modified stereomicroscope (Leica S6E) with a wavelength-controlled light source and a digital camera. Following a single injection of curcumin (7.5 mg/kg) two hours prior to imaging, curcumin-labeled plaques were visible in AD-Tg mice retina specifically at an excitation wavelength of 546/15 nm (Figure 5g - 5j). Plaques were mostly detected in areas close to the optic disc. The average plaque size was compatible with that observed in the whole-mount retina (*ex vivo*). No plaques were detected in the non-Tg (wt) mice injected i.v. with curcumin (Figure 5k) or in AD-Tg mice that did not receive curcumin injection (data not shown). To verify that the signals captured by the modified stereomicroscope originated from the plaques, mice were euthanized, and the presence of the curcumin-labeled plaques was confirmed on whole-mount retinas (data not shown).

Example 6

Mice

Double-transgenic mice (females and males at equal numbers) that harbor the chimeric mouse/human APP (APP_{swe}) and the mutant human presenilin 1 (deletion in exon 9

– PSEN1△E9) genes and their aged-matched non-Tg littermates, were purchased from the Jackson Laboratories (Bar Harbour, ME, strain #4462) and were bred and maintained in the animal center of comparative medicine of Cedars-Sinai Medical Center (Los Angeles, CA). All experiments were approved and conducted according to regulations devised by the Cedars-Sinai Institutional Animal Care and Use Committee.

Example 7

Genotyping

Genomic DNA was extracted from 0.5 cm tail tip using a DNA extraction kit (Qiagen, Valencia, CA) following the manufacturer's protocol. Mice used in this study were genotyped for the presence of the transgenes by PCR as previously described (Jankowsky, 2004, Ref. #120).

Example 8

Vaccination Preparations

Modified myelin-derived peptide (MOG45D) is derived from the encephalitogenic peptide $MOG_{(35-55)}$ (Koehler, 2002, Ref. #285; Shao, 2002, Ref. #283; Zhong, 2002, Ref. #284; Hauben, 2001, Ref. #28; and Hauben, 2001, Ref. #35). For vaccinations, MOG45D (Invitrogen, Carlsbad, CA) was added to bone marrow-derived dendritic cells from non-Tg littermates' donor mice. Preparation of dendritic cells for vaccination was as previously described (Hauben, 2003, Ref. #34).

Example 9

Experimental Regimen for Vaccinations

AD-Tg mice at the age of 7 months were injected with DC-MOG45 ($0.5x10^6$ cells/200 ml in lxPBS per animal) once a month, for three months. Control groups of 7-month-old AD-Tg mice were injected with l x PBS according to the corresponding regimens. At the end of the study, all mice were perfused under anesthesia with l x PBS following 2.5% paraformaldehyde ("PFA") (Sigma) and their brains and eyes were collected for further analysis.

Example 10

Animal Tissue

Mice were anesthetized and perfused with 4% ice-cold buffered PFA, and a group of mice were not perfused. Their eyes were enucleated and fixed immediately in 4% fresh PFA overnight. For whole mount retinas, the eyes were dissected and the anterior part was removed. The eyecups were soaked for 10 minutes in hyaluronidase (type I-S) (0.07mg/ml) (Sigma) to liquefy and remove the vitreous residues, than washed for 10 minutes x 3 in PBS, and the whole mount retinas were collected. For whole eye sectioning, the eyes were put in 30% sucrose in 4% PFA for 2 hours, than washed for 15 minutes x3 in PBS. The eyes were embedded in O.C.T and frozen slowly on dry ice than sagittal sectioned (7μm) with cryostat. Brains were collected and fixed immediately in 4% fresh PFA overnight. The brains were put in 30% sucrose (in 4% PFA) gradient. Brains were washed for 15 minutes x3 in PBS, next embedded in O.C.T and frozen slowly on dry ice, then coronal sectioned (30μm) with cryostat.

Example 11

Human Autopsy Eyes

Autopsy eyes from Alzheimer's patients were procured from the Alzheimer's Disease Research Center, Department of Pathology, University of Southern California (Los Angeles, CA), under IRB protocols 99491 and 3201. Healthy donor eyes were purchased from National Disease Research Interchange (NDRI, Philadelphia, PA). NDRI has a human tissue collection protocol approved by a managerial committee and subject to National Institutes of Health oversight. Diseased and normal eyes were fixed and stored in 10% neutral buffered formalin. In addition, we used two healthy eyes that were frozen without fixation and stored at -80oC. Whole-mount retinas were prepared from the eyes and further studied by immunohistochemistry.

Example 12

Tail Vein Injection of Curcumin

For *in* vivo Aβ-plaque imaging, AD-Tg and non-Tg wild-type mice were intravenously injected to the tail vein with curcumin in PBS (7.5mg/kg/day, for 7 consecutive days) or with PBS. Subsequently, brains and eyes were cryosectioned, or prepared for whole

mount retina. In an alternative embodiment, curcumin may be administered to the patient orally.

Example 13

Immunohistochemistry

Brain cryosections (30μm thick), retina cross sections (cryosections) (7μm thick) and whole mount retinas were treated with a permeabilization/blocking solution containing 20% horse serum (Invitrogen) and 0.01-0.1% Triton X-100 (Sigma-Aldrich, St. Louis, MO). Sections were stained overnight at 4°C with a specified combination of the following primary Abs in PBS containing 10% blocking solution: mouse anti-Aβ [human amino-acid residues 1-17; clone 6E10 (1:100; Milipore, Temecula, CA)]. The sections were incubated for 1 hour in room temperature with secondary Abs, then washed three times with 1 x PBS and mounted using Vectorshield containing or not 4',6-diamidino-2-phenylindole, dihydrochloride (DAPI, Vector Laboratories, Peterborough, UK). Secondary Abs solution in 1 x PBS contained Cy-5-conjugated donkey anti-mouse antibody (1:200; Jackson ImmunoResearch Laboratories, West Grove, PA). A negative control was processed with the same protocol with the omission of the primary antibody to assess nonspecific labeling. For microscopic analysis we used a Zeiss ApoTome fluorescent.

Example 14

Curcumin Staining

Curcumin solution at 0.1 mg/ml was prepared by dissolving curcumin (Sigma-Aldrich) in 0.5M NaOH, pH=7.9, following immediate dilution in 1 x PBS. Brain and retina tissue cryosections (30μm and 7μm thick respectively) and whole mount retinas were stained with curcumin solution for 10 minutes in room temperature, then rinsed three times with 1 x PBS for 15 minutes each. The samples were covered with GVA mounting media (Zymed).

Additional compounds are known in the art that can stain/label in vivo amyloid plaques, including, Thioflavin S and T and some derivatives, Congo Red and derivatives, methoxy-X04, Pittsburgh Compound-B (PiB), DDNP, Chrysamine-G and several more. However, curcumin and it's derivatives are very appealing for in vivo optical imaging of amyloid plaques in animal models as well as humans, because of the following advantage. Curcumin generates specific and very bright signals in the commonly used optical spectrum, and is commercially available, exceptionally low cost. Safety issues related to curcumin are

minimal (even at high dosages) and may even consider to be beneficial to the patient's health as an antioxidant. Curcumin is an effective ligand with very good in vitro and in vivo binding characteristics to Aβ, and offers good initial brain uptake and washout rate from the brain (important properties for in vivo imaging agents).

5

Example 15

Quantification

Micrographs of stained tissues were obtained on an Axio Imager Z1 ApoTome-equipped microscope (with motorized Z-drive) with AxioCam MRm monochrome camera
10 ver. 3.0 (at a resolution of 1388 x 1040 pixels, 6.45 μm x 6.45 μm pixel size, dynamic range of >1:2200, that delivers low-noise images due to Peltier-cooled sensor). Quantitative analysis of Aβ plaque number and area (βm2) was performed from two wholemounted retinas per mouse (n=4 mice per group). Each image, captured at 40x objective with resolution of 0.28 βm, included an area of 0.04 mm2, and a total of 12 rectangular areas around the optic
15 disc within scanning depth of 60 μm (multiple virtual section images at consecutive focal planes using a motorized scanning stage). Measurements of the average plaque radius (following curcumin staining) were completed for each animal group followed by calculation of the average plaque area in each animal group. For the acquisition, we used similar exposure times (approx. 75 ms) and the same gain values (0) for all images. No image post-
20 processing was preformed. The emission signals of Aβplaques stained with curcumin were compared to the background signals in the retinal tissue, to determine signal to background ratio. The calculated signal-to-background noise ratio from the images was high and within the range of 3:1 to 10:1. Quantitative analysis of Aβ plaque number and area (βm2) in the brain was determined from three coronal sections (two hemispheres each) per mouse with
25 450 μm intervals, over an area covering hippocampal and cortical regions. Optical sections from each field of the specimen were imported into the NIH Image J program (National Institutes of Health). Conversion to greyscale was performed to distinguish between areas of immunoreactivity and background. Total area and quantitative levels of immunoreactivity were determined using a standardized custom histogram-based threshold technique, and then
30 subjected to particle analysis.

Example 16

Spectral and Multispectral Imaging.

Spectral imaging provides digital images of an object at a large, sequential number of wavelengths generating precise optical signatures at every pixel. The fluorescence spectral signature of Aβ plaques, labeled *in vivo* with curcumin, was captured by our spectral imaging system using the following equipment: Nikon fluorescence microscopes (E800 and TE2000), mercury and xenon arc lamps, a CCD camera, an AOTF (acousto-optic tunable filters)-based spectral image acquisition system (ChromoDynamics, Inc)[29] and post-analysis imaging software developed by our Minimally Invasive Surgical Technologies Institute [30]. The final images provided a visual pseudo-color representation of the spectral signature extracted from the raw images, representing the size and location of the analyzed objects. In multispectral imaging, fluorescence lifetime imaging, performed with a pulsed laser and a LaVision PicoStar HR gated camera, was supplementing the spectral acquisition.

Figure 6 depicts a flow diagram of a spectral imaging system 100 for diagnosing, prognosing, and analyzing Aβ plaques *in vivo* in accordance with an embodiment of the present invention. The subject matter retina 110 is stained with a fluorescent marker to label Aβ plaques. Shortly thereafter, the stained retina 110 is imaged by an imaging device 120 that is adjusted to visualize fluorescence and scatter signals at higher resolutions. The imaging device 120 may be fitted with a Polychrome V variable spectral light source 130. In additional embodiments, the spectral imaging system 100 may incorporate a color digital camera 140 (e.g. MicroFire) and one or more magnifying lenses to improve magnification and image detail. Image acquisition 170 is attained by post-analysis image segmentation and classification using imaging software 160.

Figure 7 depicts a flow diagram of a spectral imaging system 200 for diagnosing, prognosing, and analyzing Aβ plaques in accordance with an embodiment of the present invention. The subject matter retina 210 is stained with a fluorescent marker to label Aβ plaques. Shortly thereafter, the stained retina 210 is imaged using an imaging device 220. The imaging device 220 may be fitted with multi-spectral imaging technology, comprising of spectral imaging with acousto-optic tunable filters (AOTF) 230 and fluorescence lifetime imaging using a digital camera 240. Image acquisition 260 is attained by post-analysis image segmentation and classification using imaging software 250.

Example 17

In-Vivo Imaging of Mouse Retina.

AD-Tg and wt mice retinas were imaged two hours following curcumin intravenous injection. Mice were anaesthetized with Ketamine 100mg/ml/kg and Xylazine 20mg/ml/kg. Mouse pupils were dilated to about 2mm in diameter with 0.5% phenylephrine hydrochloride ophthalmic solution (Bausch & Lomb) combined with 0.5% tropicamide ophthalmic solution (Mydral; Bausch & Lomb). During the imaging process, the mice were positioned on a stage of the stereomicroscope, and the eye was covered with a drop of PBS supplemented with calcium and magnesium, which served as an optical coupling medium between the eye surface and the imaging lens. A modified stereomicroscope (Leica S6E) that was adjusted to visualize fluorescence and scatter signals at higher resolution was used to capture images (exposure time 750 ms. with gain 4). The modified stereomicroscope was assembled to include a Polychrome V (Till Photonics) variable wavelength light source, a MicroFire color digital camera (Optronics), and an additional 6x (double convex) magnifying lens, with a focal length of 10 cm. Images were repeatedly captured at several different angles, in order to visualize a larger field and to eliminate non-specific reflection signals.

Example 18

Statistical Analysis

Results were analyzed by one tailed unpaired Student's *t* test for the p values of two-group comparison. Results are expressed as means ± SD.

Various embodiments of the present subject matter are described above in the Detailed Description. While these descriptions directly describe the above embodiments, it is understood that those skilled in the art may conceive modifications and/or variations to the specific embodiments shown and described herein. Any such modifications or variations that fall within the purview of this description are intended to be included therein as well. Unless specifically noted, it is the intention of the inventors that the words and phrases in the specification and claims be given the ordinary and accustomed meanings to those of ordinary skill in the applicable art(s).

The foregoing description of various embodiments of the present subject matter known to the applicant at this time of filing the application has been presented and is intended for the purposes of illustration and description. The present description is not intended to be exhaustive nor limit the subject matter to the precise form disclosed and many modifications

and variations are possible in the light of the above teachings. The embodiments described serve to explain the principles of the present subject matter and its practical application and to enable others skilled in the art to utilize the subject matter in various embodiments and with various modifications as are suited to the particular use contemplated. Therefore, it is intended that the present subject matter not be limited to the particular embodiments disclosed for carrying out the subject matter.

While particular embodiments of the present subject matter have been shown and described, it will be obvious to those skilled in the art that, based upon the teachings herein, changes and modifications may be made without departing from this subject matter and its broader aspects and, therefore, the appended claims are to encompass within their scope all such changes and modifications as are within the true spirit and scope of this subject matter. It will be understood by those within the art that, in general, terms used herein are generally intended as "open" terms (*e.g.*, the term "including" should be interpreted as "including but not limited to," the term "having" should be interpreted as "having at least," the term "includes" should be interpreted as "includes but is not limited to," etc.).

References

1. Sisodia, S.S. & Price, D.L. Role of the beta-amyloid protein in Alzheimer's disease. *FASEB J* 9, 366-370 (1995).
2. Hardy, J. & Selkoe, D.J. The amyloid hypothesis of Alzheimer's disease: progress and problems on the road to therapeutics. *Science* 297, 353-356 (2002).
3. McGeer, P.L. & McGeer, E.G. Local neuroinflammation and the progression of Alzheimer's disease. *J Neurovirol* 8, 529-538 (2002).
4. Klunk, W.E. et al. Imaging brain amyloid in Alzheimer's disease with Pittsburgh Compound-B. *Ann Neurol* 55, 306-319 (2004).
5. Ng, S. et al. Visual assessment versus quantitative assessment of 11C-PIB PET and 18F-FDG PET for detection of Alzheimer's disease. *J Nucl Med* 48, 547-552 (2007).
6. Wang, Y. et al. Development of a PET/SPECT agent for amyloid imaging in Alzheimer's disease. *J Mol Neurosci* 24, 55-62 (2004).
7. Nordberg, A. Amyloid plaque imaging in vivo: current achievement and future prospects. *Eur J Nucl Med Mol Imaging* 35 Suppl 1, S46-50 (2008).
8. Hintersteiner, M. et al. In vivo detection of amyloid-beta deposits by near-infrared imaging using an oxazine-derivative probe. *Nat Biotechnol* 23, 577-583 (2005).
9. Nakada, T., Matsuzawa, H., Igarashi, H., Fujii, Y. & Kwee, I.L. In vivo visualization of senile-plaque-like pathology in Alzheimer's disease patients by MR microscopy on a 7T system. *J Neuroimaging* 18, 125-129 (2008).
10. Toyama, H. et al. PET imaging of brain with the beta-amyloid probe, [11C]6-OHBTA- 1, in a transgenic mouse model of Alzheimer's disease. *Eur J Nucl Med Mol Imaging* 32, 593-600 (2005).
11. Klunk, W.E. et al. Binding of the positron emission tomography tracer Pittsburgh compound-B reflects the amount of amyloid-beta in Alzheimer's disease brain but not in transgenic mouse brain. *J Neurosci* 25, 10598-10606 (2005).
12. Lockhart, A. et al. PIB is a non-specific imaging marker of amyloid-beta (Abeta) peptide-related cerebral amyloidosis. *Brain* 130, 2607-2615 (2007).
13. Meyer-Luehmann, M. et al. Rapid appearance and local toxicity of amyloid-beta plaques in a mouse model of Alzheimer's disease. *Nature* 451, 720-724 (2008).
14. Morin, P.J. et al. Amyloid precursor protein is synthesized by retinal ganglion cells, rapidly transported to the optic nerve plasma membrane and nerve terminals, and metabolized. *J Neurochem* 61, 464-473 (1993).

15. Greeve, I. et al. Age-dependent neurodegeneration and Alzheimer-amyloid plaque formation in transgenic Drosophila. *J Neurosci* 24, 3899-3906 (2004).

16. Ning, A., Cui, J.Z., To, E., Hsiao Ashe, K. & Matsubara, J.A. Amyloid Beta Deposits Lead to Retinal Degeneration in a Mouse Model of Alzheimer Disease. *Invest Ophthalmol Vis Sci* (2008).

17. Koronyo-Hamaoui, M. et al. Dendritic-cell based vaccination with a weak agonist of myelin-derived peptide attenuates Alzheimer's-like pathology in APP/PS1 transgenic mice. *SfN abstract 740.1/Q1* (2008).

18. Hauben, E. et al. Vaccination with dendritic cells pulsed with peptides of myelin basic protein promotes functional recovery from spinal cord injury. *J Neurosci* 23, 8808- 8819 (2003).

19. Yang, F. et al. Curcumin inhibits formation of amyloid beta oligomers and fibrils, binds plaques, and reduces amyloid in vivo. *J Biol Chem* 280, 5892-5901 (2005).

20. Garcia-Alloza, M., Borrelli, L.A., Rozkalne, A., Hyman, B.T. & Bacskai, B.J. Curcumin labels amyloid pathology in vivo, disrupts existing plaques, and partially 18 restores distorted neurites in an Alzheimer mouse model. *J Neurochem* 102, 1095- 1104 (2007).

21. Schnell, S.A., Staines, W.A. & Wessendorf, M.W. Reduction of lipofuscin-like autofluorescence in fluorescently labeled tissue. *J Histochem Cytochem* 47, 719-730 (1999).

22. Baschong, W., Suetterlin, R. & Laeng, R.H. Control of autofluorescence of archival formaldehyde-fixed, paraffin-embedded tissue in confocal laser scanning microscopy (CLSM). *J Histochem Cytochem* 49, 1565-1572 (2001).

23. Garcia-Alloza, M. et al. Characterization of amyloid deposition in the APPswe/PS1dE9 mouse model of Alzheimer disease. *Neurobiol Dis* 24, 516-524 (2006).

24. Frenkel, D., Maron, R., Burt, D.S. & Weiner, H.L. Nasal vaccination with a proteosome-based adjuvant and glatiramer acetate clears beta-amyloid in a mouse model of Alzheimer disease. *J Clin Invest* 115, 2423-2433 (2005).

25. Butovsky, O. et al. Glatiramer acetate fights against Alzheimer's disease by inducing dendritic-like microglia expressing insulin-like growth factor 1. *Proc Natl Acad Sci U S A* 103, 11784-11789 (2006).

26. Butovsky, O., Kunis, G., Koronyo-Hamaoui, M. & Schwartz, M. Selective ablation of bone marrow-derived dendritic cells increases amyloid plaques in a mouse Alzheimer's disease model. *Eur J Neurosci* 26, 413-416 (2007).

27. Ford, M.L. & Evavold, B.D. An MHC anchor-substituted analog of myelin oligodendrocyte glycoprotein 35-55 induces IFN-gamma and autoantibodies in the absence of experimental autoimmune encephalomyelitis and optic neuritis. *Eur J Immunol* 34, 388-397 (2004).

28. Ziv, Y., Avidan, H., Pluchino, S., Martino, G. & Schwartz, M. Synergy between immune cells and adult neural stem/progenitor cells promotes functional recovery from spinal cord injury. *Proc Natl Acad Sci U S A* 103, 13174-13179 (2006).

29. Wachman, E.S., Niu, W. & Farkas, D.L. AOTF microscope for imaging with increased speed and spectral versatility. *Biophys J* 73, 1215-1222 (1997).

30. Burton, K., Jeong, J., Wachsmann-Hogiu, S. and Farkas, D. L. Spectral optical imaging in biology and medicine in Biomedical Optical Imaging, Edn. In press. (Oxford University Press 2008).

31. Goldstein, L.E. et al. Cytosolic beta-amyloid deposition and supranuclear cataracts in lenses from people with Alzheimer's disease. *Lancet* 361, 1258-1265 (2003).

32. Carroll, J., Choi, S.S. & Williams, D.R. In vivo imaging of the photoreceptor mosaic of a rod monochromat. *Vision Res* 48, 2564-2568 (2008).

33. Murata, H. et al. Imaging mouse retinal ganglion cells and their loss in vivo by a fundus camera in the normal and ischemia-reperfusion model. *Invest Ophthalmol Vis Sci* 49, 5546-5552 (2008).

34. Leung, C.K. et al. Longitudinal profile of retinal ganglion cell damage after optic nerve crush with blue-light confocal scanning laser ophthalmoscopy. *Invest Ophthalmol Vis Sci* 49, 4898-4902 (2008).

35. Dhillon, N. et al. Phase II trial of curcumin in patients with advanced pancreatic cancer. *Clin Cancer Res* 14, 4491-4499 (2008).

36. Anand, P., Kunnumakkara, A.B., Newman, R.A. & Aggarwal, B.B. Bioavailability of curcumin: problems and promises. *Mol Pharm* 4, 807-818 (2007).

37. Sadun, A.A., Borchert, M., DeVita, E., Hinton, D.R. & Bassi, C.J. Assessment of visual impairment in patients with Alzheimer's disease. *Am J Ophthalmol* 104, 113- 120 (1987).

38. Katz, B. & Rimmer, S. Ophthalmologic manifestations of Alzheimer's disease. *Surv Ophthalmol* 34, 31-43 (1989).

39. Hinton, D.R., Sadun, A.A., Blanks, J.C. & Miller, C.A. Optic-nerve degeneration in Alzheimer's disease. *N Engl J Med* 315, 485-487 (1986).

40. Blanks, J.C., Torigoe, Y., Hinton, D.R. & Blanks, R.H. Retinal pathology in Alzheimer's disease. I. Ganglion cell loss in foveal/parafoveal retina. *Neurobiol Aging* 17, 377-384 (1996).

41. Trick, G.L., Barris, M.C. & Bickler-Bluth, M. Abnormal pattern electroretinograms in patients with senile dementia of the Alzheimer type. *Ann Neurol* 26, 226-231 (1989).

42. Katz, B., Rimmer, S., Iragui, V. & Katzman, R. Abnormal pattern electroretinogram in Alzheimer's disease: evidence for retinal ganglion cell degeneration? *Ann Neurol* 26, 221-225 (1989).

43. Parisi, V. et al. Morphological and functional retinal impairment in Alzheimer's disease patients. *Clin Neurophysiol* 112, 1860-1867 (2001).

44. Berisha, F., Feke, G.T., Trempe, C.L., McMeel, J.W. & Schepens, C.L. Retinal abnormalities in early Alzheimer's disease. *Invest Ophthalmol Vis Sci* 48, 2285-2289 (2007).

45. Anderson, D.H. et al. Characterization of beta amyloid assemblies in drusen: the deposits associated with aging and age-related macular degeneration. *Exp Eye Res* 78, 243-256 (2004).

46. Dentchev, T., Milam, A.H., Lee, V.M., Trojanowski, J.Q. & Dunaief, J.L. Amyloidbeta is found in drusen from some age-related macular degeneration retinas, but not in drusen from normal retinas. *Mol Vis* 9, 184-190 (2003).

47. Ding, J.D. et al. Targeting age-related macular degeneration with Alzheimer's disease based immunotherapies: anti-amyloid-beta antibody attenuates pathologies in an agerelated macular degeneration mouse model. *Vision Res* 48, 339-345 (2008).

48. Koronyo, Y., Koronyo-Hamaoui, M., Black, K.L., Schwartz, M. & Farkas, D.L., Optical method for the detection of Alzheimer's Disease. Patent application submitted to the USPTO (2008)

49. Jankowsky, J.L. et al. APP processing and amyloid deposition in mice haploinsufficient for presenilin 1. *Neurobiol Aging* 25, 885-892 (2004).

50. McKinnon SJ, Lehman DM, Kerrigan-Baumrind LA, Merges CA, Pease ME, Kerrigan DF, Ransom NL, Tahzib NG, Reitsamer HA, Levkovitch-Verbin H, *et al.* (2002) *Invest Ophthalmol Vis Sci* 43, 1077-1087.

51. Yoneda S, Hara H, Hirata A, Fukushima M, Inomata Y, & Tanihara H (2005) *Jpn J Ophthalmol* 49, 106-108.

52. Guo L, Salt TE, Luong V, Wood N, Cheung W, Maass A, Ferrari G, Russo-Marie F, Sillito AM, Cheetham ME, *et al.* (2007) *Proc Natl Acad Sci U S A* 104, 13444-

13449.

53. Dentchev T, Milam AH, Lee VM, Trojanowski JQ, & Dunaief JL (2003) *Mol Vis* 9, 184-190.

CLAIMS

WHAT IS CLAIMED IS:

1. A method of diagnosing Alzheimer's disease in a mammal, comprising:

administering a fluorescent marker to the mammal for staining Aβ peptides;

imaging the mammal's retina with an optical imaging system;

examining the images for stained Aβ peptides; and

diagnosing the mammal as having Alzheimer's disease if stained Aβ peptides are present.

2. The method of claim 1, wherein the optical imaging is performed *in vivo*.

3. The method of claim 1, wherein the fluorescent marker is selected from the group consisting of curcumin, curcumin derivatives, Thioflavin S and derivatives, Thioflavin T and derivatives, Congo Red and derivatives, methoxy-X04, Pittsburgh Compound-B (PiB), DDNP, Chrysamine-G, and combinations thereof.

4. The method of claim 1, wherein the optical imaging system is selected from the group consisting of a spectrometer, a fluorescence microscope, a stereomicroscope, a mercury arc lamp, a variable wavelength light source, a xenon arc lamp, a CCD gated camera, a color digital camera, an acoustic-optic tunable filter–based spectral image acquisition system, adaptive optics, imaging software, and combinations thereof.

5. The method of claim 3, wherein the fluorescent marker is curcumin and the amount of curcumin administered is less than 12.0 grams and greater 7.5 mg.

6. A method of prognosing Alzheimer's disease in a mammal, comprising:

administering a fluorescent marker to the subject for staining Aβ peptides;

imaging the subject's retina with an optical imaging system;

examining the images for stained Aβ peptides;

quantitating the increase/decrease of stained Aβ peptides in the subject's retina, as compared to a prior diagnosis; and

rendering a prognosis based upon the level of stained Aβ peptides in the subject's retina.

7. The method of claim 6, wherein the optical imaging is performed *in vivo*.

8. The method of claim 6, wherein the fluorescent marker is selected from the group consisting of curcumin, curcumin derivatives, Thioflavin S and derivatives, Thioflavin T and derivatives, Congo Red and derivatives, methoxy-X04, Pittsburgh Compound-B (PiB), DDNP, Chrysamine-G, and combinations thereof.

9. The method of claim 6, wherein the optical imaging system is selected from the group consisting of a spectrometer, a fluorescence microscope, a stereomicroscope, a mercury arc lamp, a variable wavelength light source, a xenon arc lamp, a CCD gated camera, a color digital camera, an acoustic-optic tunable filter–based spectral image acquisition system, adaptive optics, imaging software, and combinations thereof.

10. The method of claim 8, wherein the fluorescent marker is curcumin and the amount of curcumin administered is less than 12.0 grams and greater 7.5 mg.

11. A method of identifying Aβ peptides in a mammal's retina, comprising:

administering a fluorescent marker to the mammal for staining the Aβ peptides;

imaging the mammal's retina with an optical imaging system; and

examining the images for stained Aβ peptides.

12. The method of claim 11, wherein the optical imaging is performed *in vivo*.

13. The method of claim 11, wherein the fluorescent marker is selected from the group consisting of curcumin, curcumin derivatives, Thioflavin S and derivatives, Thioflavin T and derivatives, Congo Red and derivatives, methoxy-X04, Pittsburgh Compound-B (PiB), DDNP, Chrysamine-G, and combinations thereof.

14. The method of claim 11, wherein the optical imaging system is selected from the group consisting of a spectrometer, a fluorescence microscope, a stereomicroscope, a mercury arc lamp, a variable wavelength light source, a xenon arc lamp, a CCD gated camera, a color digital camera, an acoustic-optic tunable filter–based spectral image acquisition system, adaptive optics, imaging software, and combinations thereof.

15. The method of claim 13, wherein the fluorescent marker is curcumin and the amount of curcumin administered is less than 12.0 grams and greater 7.5 mg.

16. A method of treating Alzheimer's disease in a mammal, comprising:

providing a therapeutically effective amount of myelin-derived peptides and/or agonist of myelin-derived peptides; and

administering the therapeutically effective amount of myelin-derived peptides and/or agonist of myelin-derived peptides to the mammal.

17. A method of evaluating the effectiveness of Alzheimer's disease treatment in a mammal comprising:

administering a fluorescent marker to the mammal for staining Aβ peptides;

imaging the mammal's retina with an optical imaging system;

examining the images for stained Aβ peptides; and

evaluating the effectiveness of Alzheimer's disease treatment based upon the level of stained Aβ peptides in the mammal's retina.

18. The method of claim 17, wherein the optical imaging is performed *in vivo*.

19. The method of claim 17, wherein the fluorescent marker is selected from the group consisting of curcumin, curcumin derivatives, Thioflavin S and derivatives, Thioflavin T and derivatives, Congo Red and derivatives, methoxy-X04, Pittsburgh Compound-B (PiB), DDNP, Chrysamine-G, and combinations thereof.

20. The method of claim 17, wherein the optical imaging system is selected from the group consisting of a spectrometer, a fluorescence microscope, a stereomicroscope, a mercury arc lamp, a variable wavelength light source, a xenon

arc lamp, a CCD gated camera, a color digital camera, an acoustic-optic tunable filter–based spectral image acquisition system, adaptive optics, imaging software, and combinations thereof.

21. The method of claim 19, wherein the fluorescent marker is curcumin and the amount of curcumin administered is less than 12.0 grams and greater 7.5 mg.

22. A method of treating a retinal ailment associated with Aβ peptides in a mammal, comprising:

providing a therapeutically effective amount of myelin-derived peptides and/or agonist of myelin-derived peptides; and

administering a therapeutically effective amount of the myelin-derived peptides and/or agonist of myelin-derived peptides to the mammal.

23. A method of evaluating the effectiveness of treatment for an Aβ peptide associated retinal ailment in a mammal comprising:

administering a fluorescent marker to the mammal for staining Aβ peptides;

imaging the mammal's retina with an optical imaging system;

examining the images for stained Aβ peptides; and

evaluating the effectiveness of treatment for the Aβ peptide associated retinal ailment based upon the level of stained Aβ peptides in the mammal's retina.

24. The method of claim 23, where in the retinal ailment is selected from a group consisting of vision loss, cataracts, glaucoma, aged-related macular degeneration, neurodegenerative conditions in which amyloid plaques are accumulated in the retina, and combinations thereof.

25. The method of claim 22, wherein the optical imaging is performed *in vivo*.

26. The method of claim 22, wherein the fluorescent marker is selected from the group consisting of curcumin, curcumin derivatives, Thioflavin S and derivatives, Thioflavin T and derivatives, Congo Red and derivatives, methoxy-X04, Pittsburgh Compound-B (PiB), DDNP, Chrysamine-G, and combinations thereof.

27. The method of claim 22, wherein the optical imaging system is selected from the group consisting of a spectrometer, a fluorescence microscope, a stereomicroscope, a mercury arc lamp, a variable wavelength light source, a xenon arc lamp, a CCD gated camera, a color digital camera, an acoustic-optic tunable filter–based spectral image acquisition system, adaptive optics, imaging software, and combinations thereof.

28. The method of claim 26, wherein the fluorescent marker is curcumin and the amount of curcumin administered is less than 12.0 grams and greater 7.5 mg.

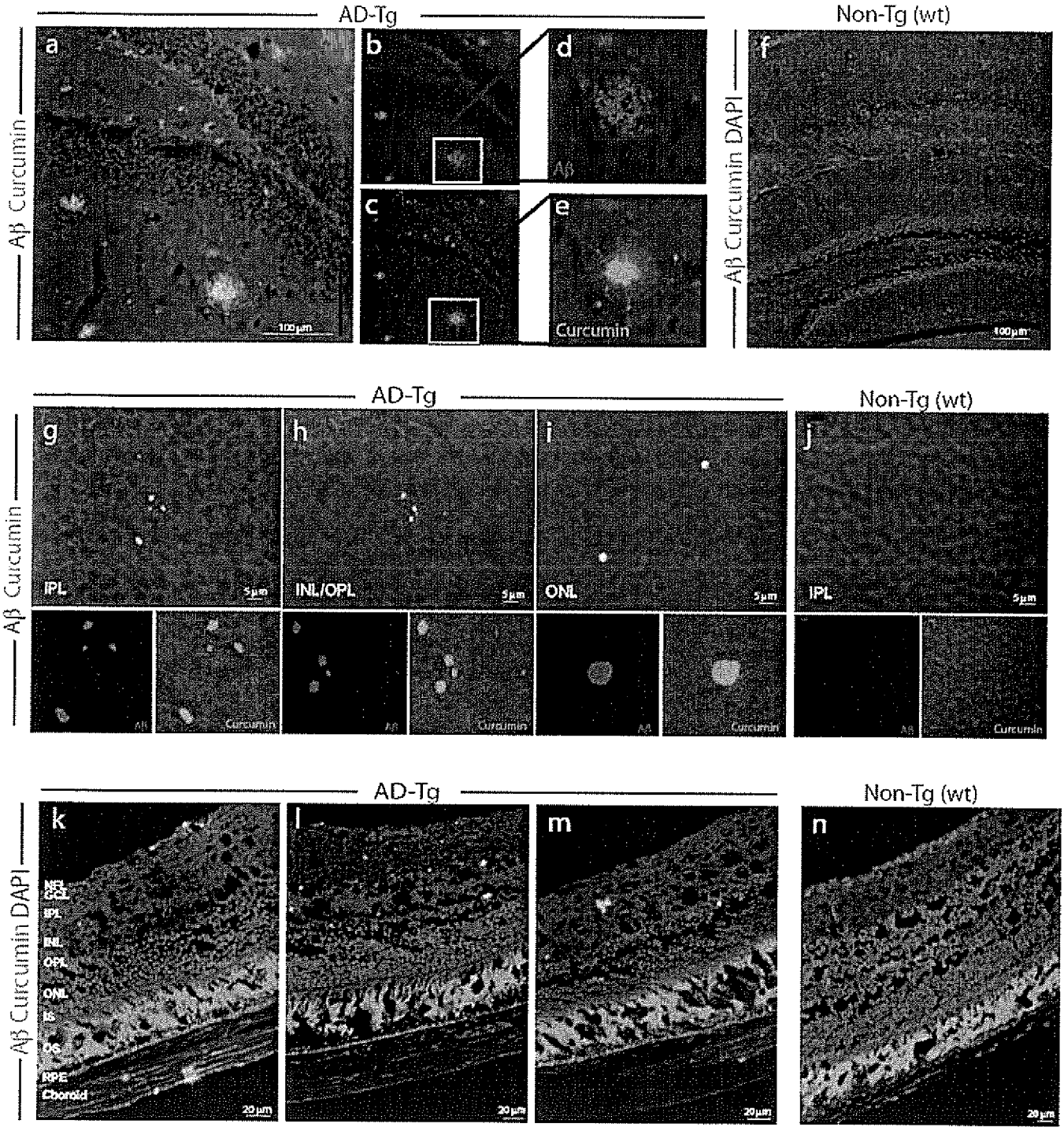
AD-Tg
Non-Tg (wt)
Aβ Curcumin
Aβ Curcumin DAPI
a
b
c
d
e
f
Aβ
Curcumin
100μm
AD-Tg
Non-Tg (wt)
Aβ Curcumin
g
h
i
j
IPL
INL/OPL
ONL
IPL
5μm
Aβ
Curcumin
AD-Tg
Non-Tg (wt)
Aβ Curcumin DAPI
k
l
m
n
NFL
GCL
IPL
INL
OPL
ONL
IS
OS
RPE
Choroid
20μm

Figure 1

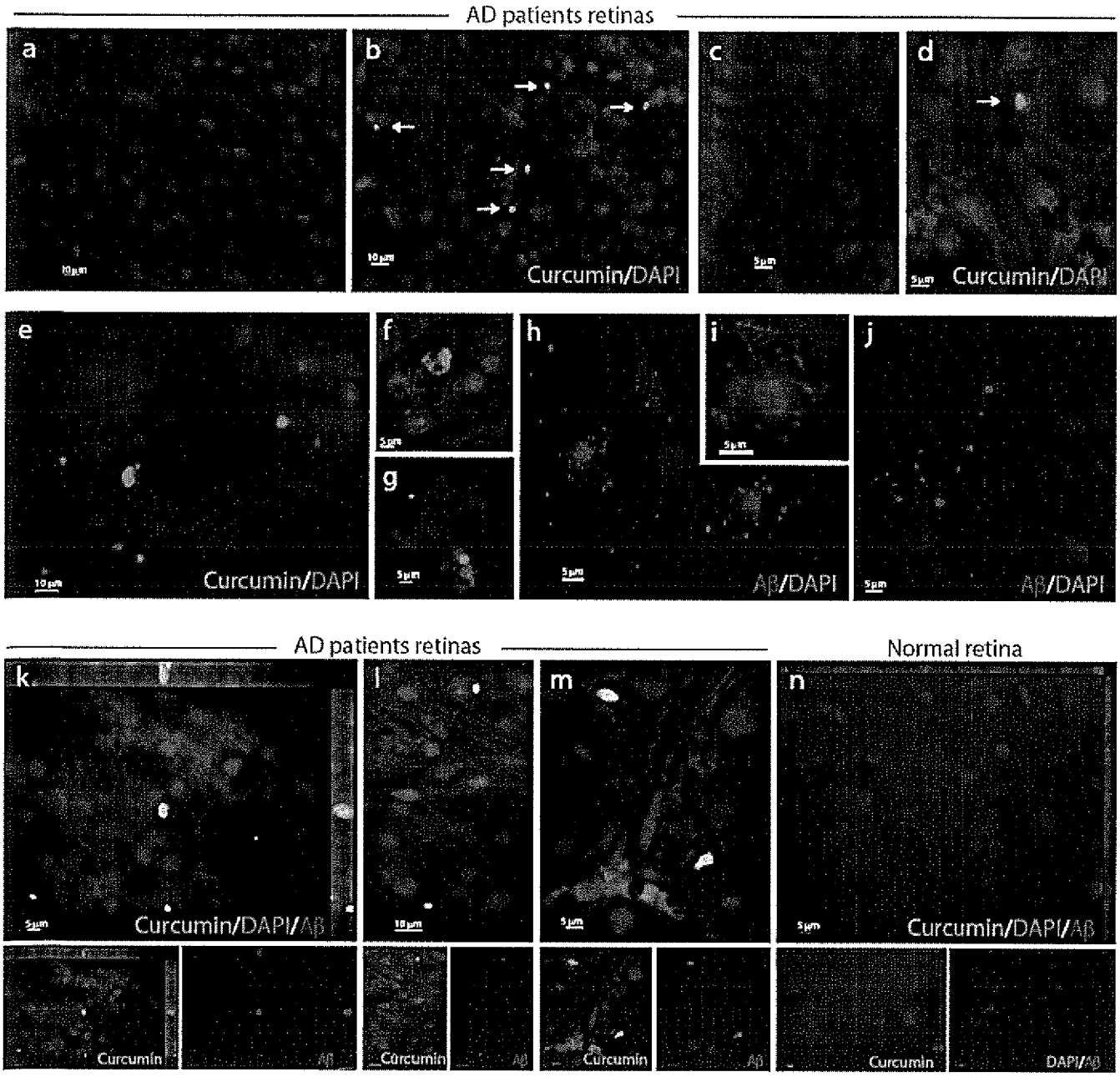
AD patients retinas
a
b
Curcumin/DAPI
c
d
Curcumin/DAPI
e
Curcumin/DAPI
f
g
h
Aβ/DAPI
i
j
Aβ/DAPI
AD patients retinas
Normal retina
k
Curcumin/DAPI/Aβ
l
m
n
Curcumin/DAPI/Aβ
Curcumin
Aβ
Curcumin
Aβ
Curcumin
Aβ
Curcumin
DAPI/Aβ

Figure 2

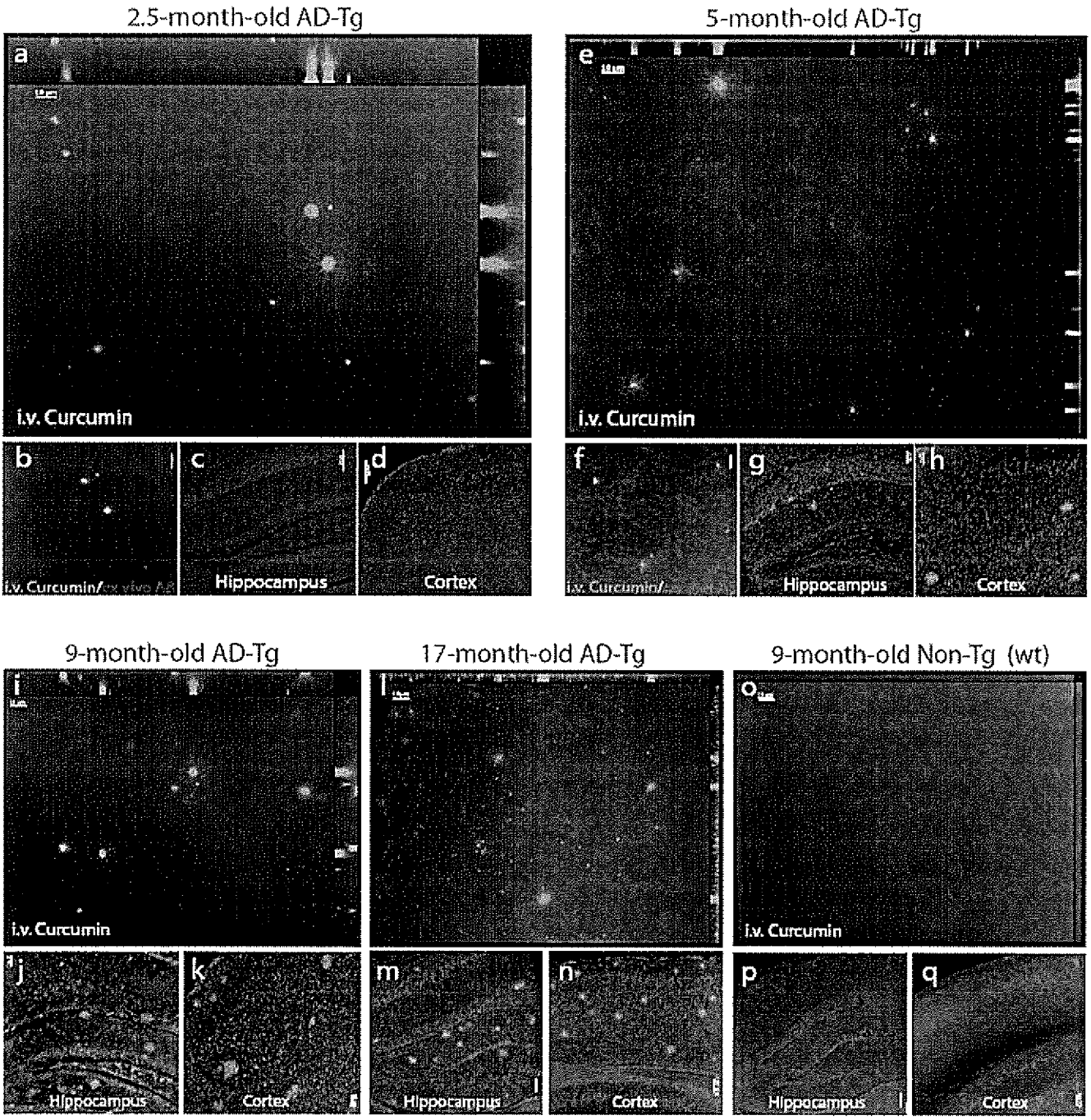
2.5-month-old AD-Tg
5-month-old AD-Tg
a
i.v. Curcumin
e
i.v. Curcumin
b
c
d
Hippocampus
Cortex
f
g
h
Hippocampus
Cortex
9-month-old AD-Tg
17-month-old AD-Tg
9-month-old Non-Tg (wt)
i
i.v. Curcumin
l
o
i.v. Curcumin
j
k
m
n
p
q
Hippocampus
Cortex
Hippocampus
Cortex
Hippocampus
Cortex

Figure 3

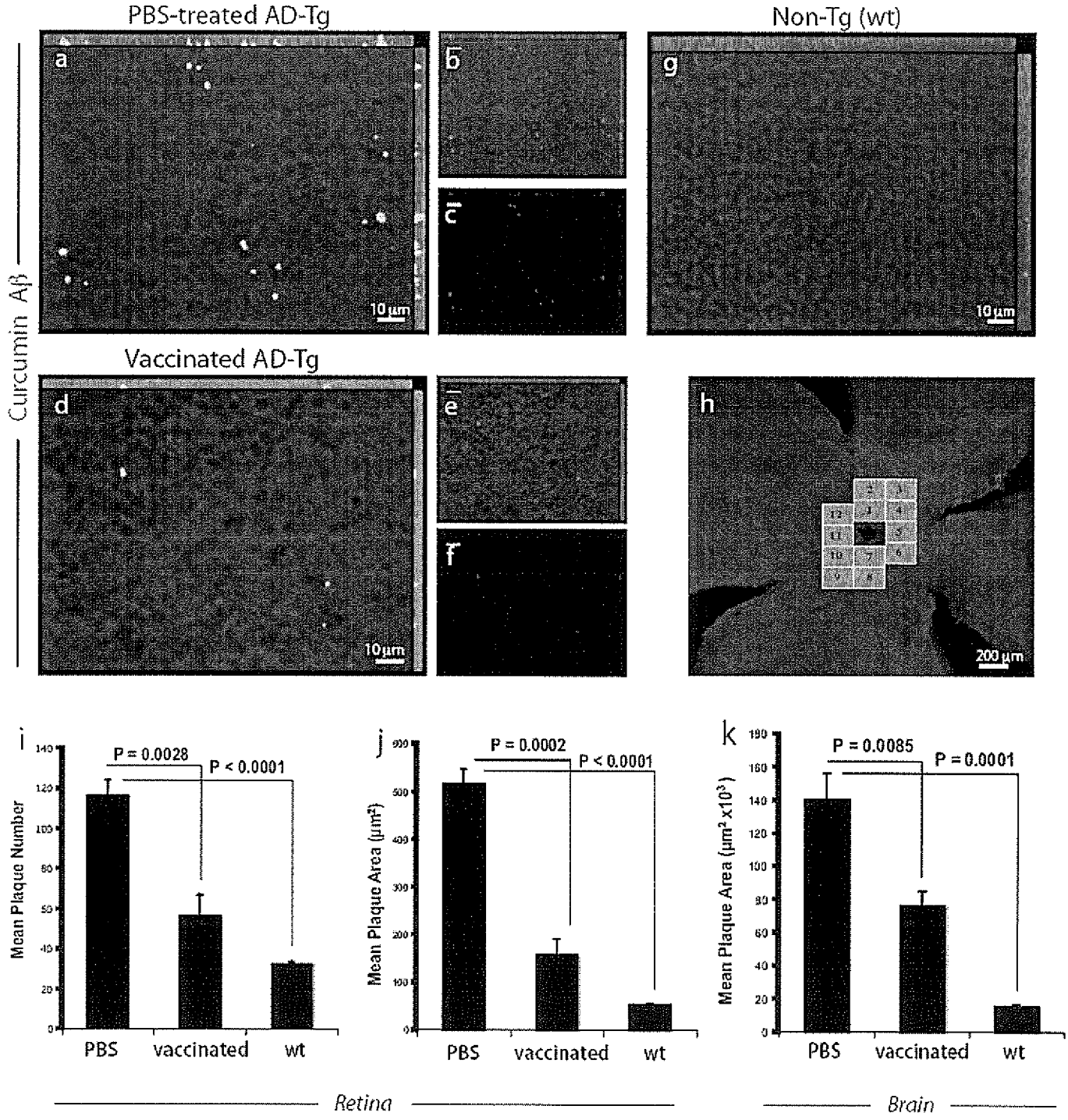
PBS-treated AD-Tg
Non-Tg (wt)
Vaccinated AD-Tg
Curcumin Aβ
a
b
c
d
e
f
g
h
10 µm
200 µm
i
j
k
P = 0.0028
P < 0.0001
P = 0.0002
P < 0.0001
P = 0.0085
P = 0.0001
Mean Plaque Number
Mean Plaque Area (µm²)
Mean Plaque Area (µm² x10³)
PBS
vaccinated
wt
Retina
Brain

Figure 4

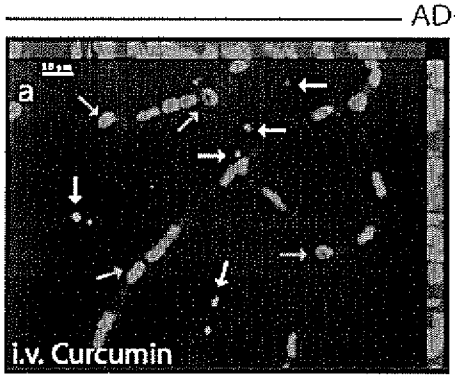

Figure 5a

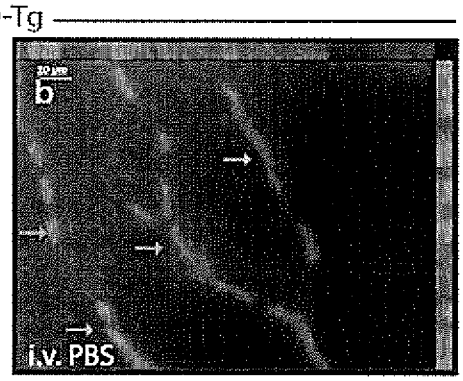

Figure 5b

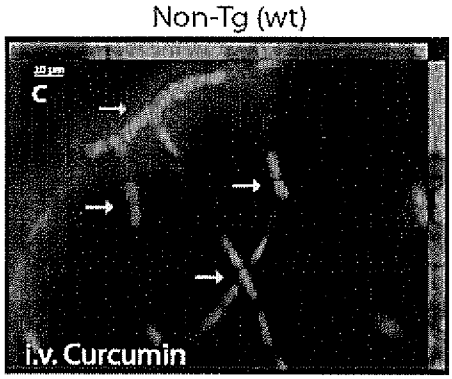

Figure 5c

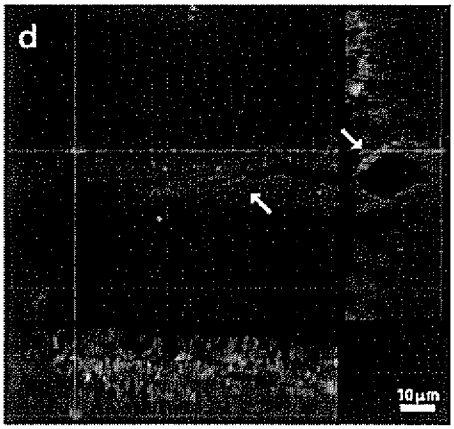

Figure 5d

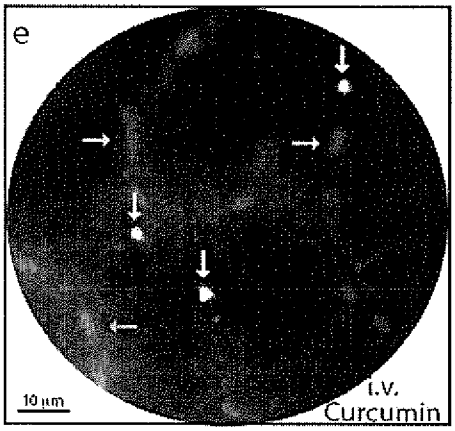

Figure 5e

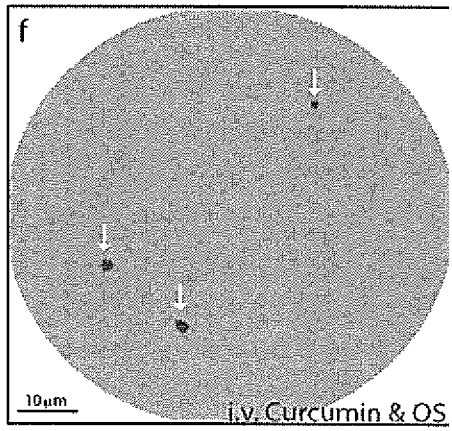

Figure 5f

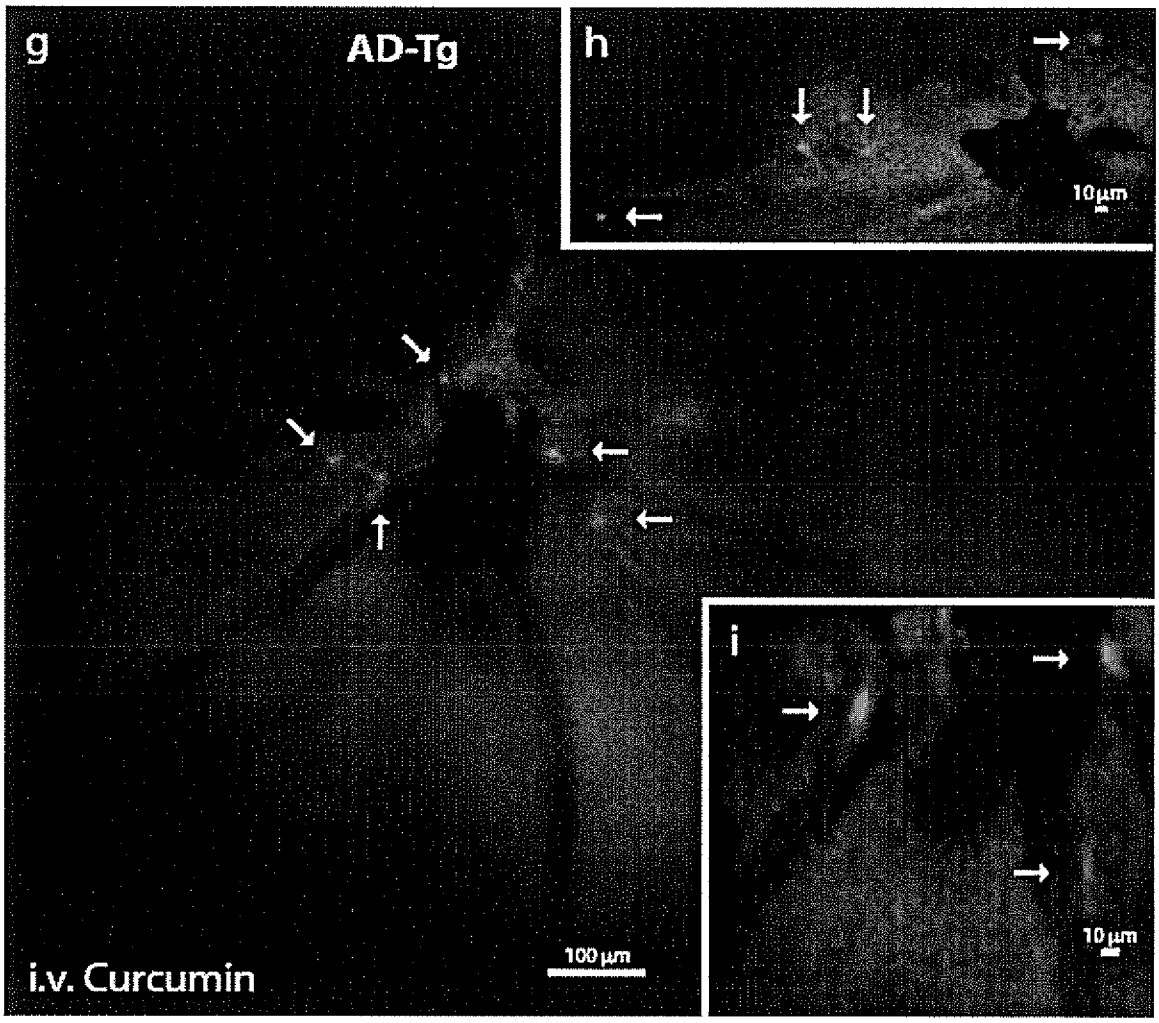

Figures 5g, 5h and 5i

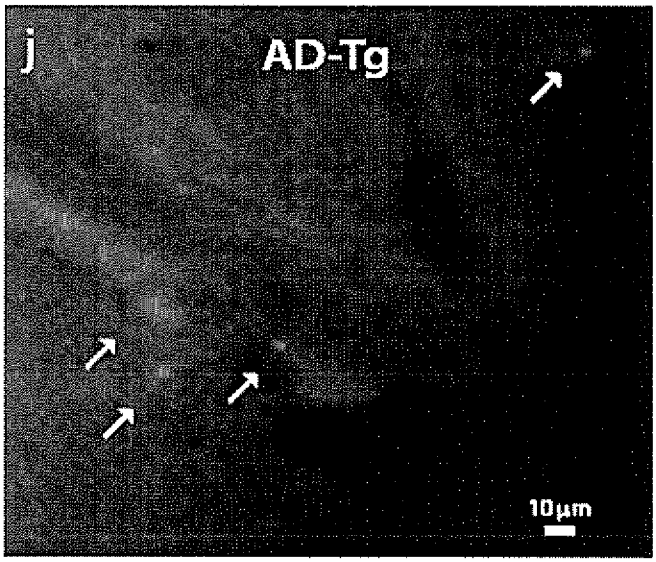

Figure 5j

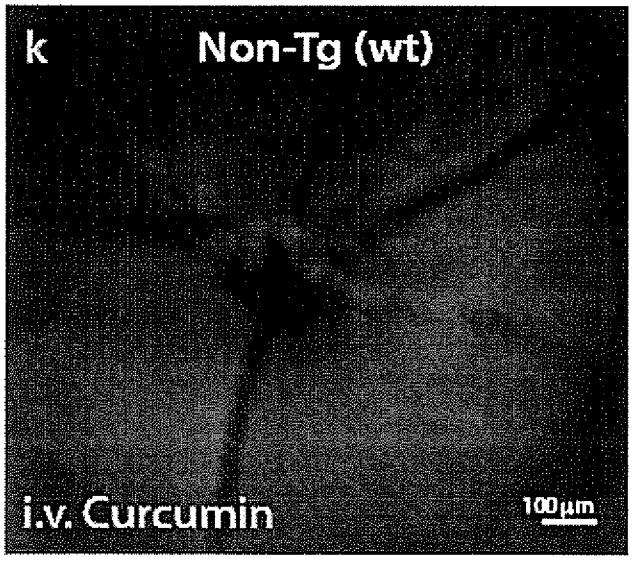

Figure 5k

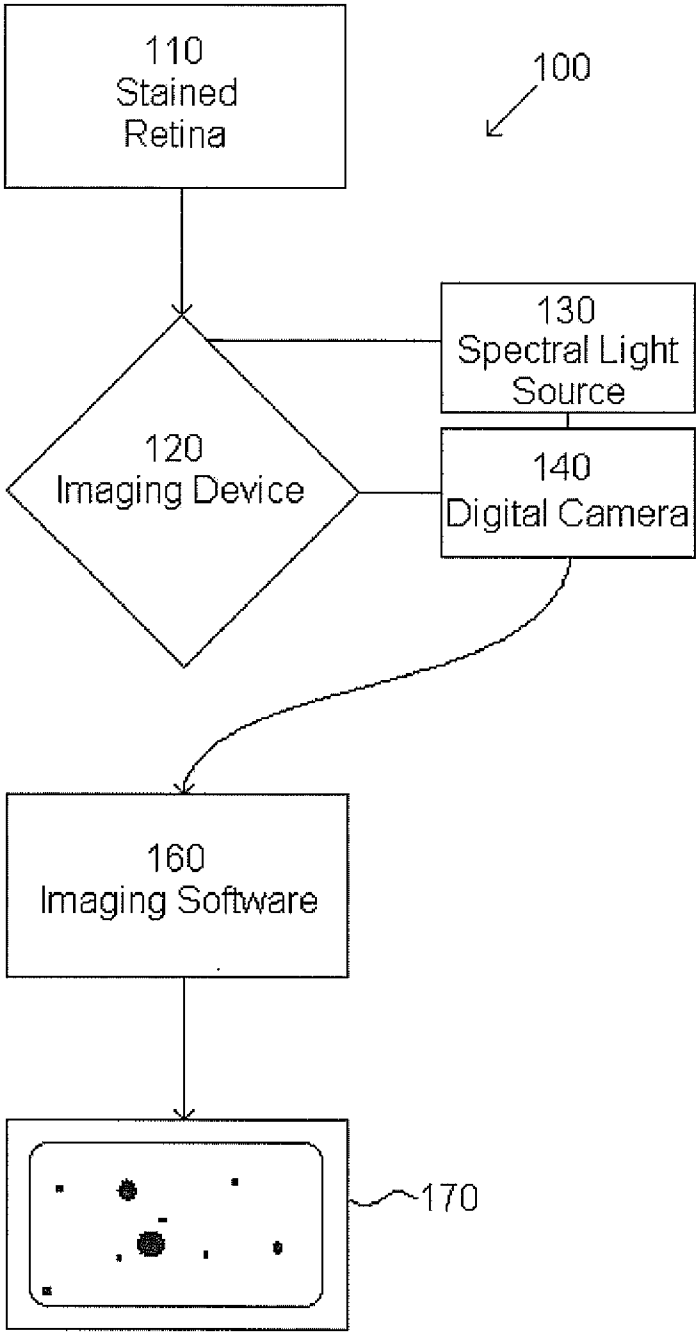
110
Stained
Retina
100
130
Spectral Light
Source
120
Imaging Device
140
Digital Camera
160
Imaging Software
170

Figure 6

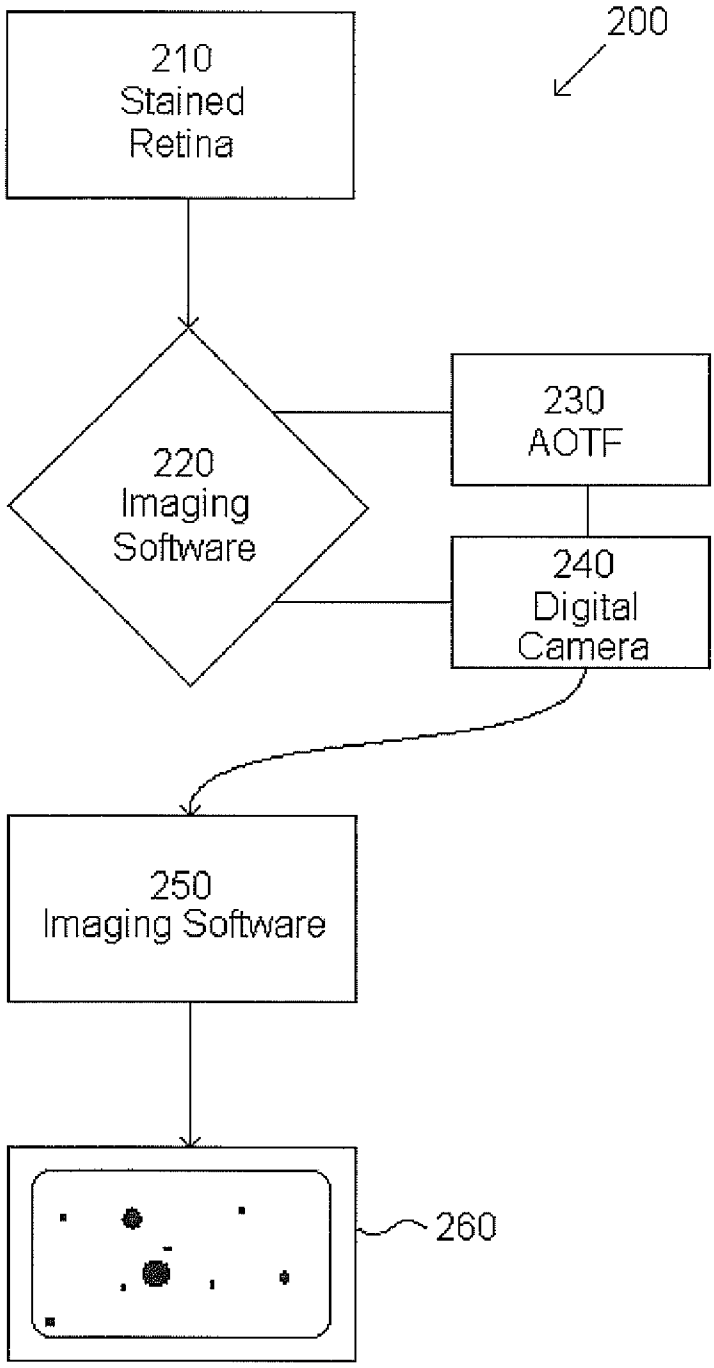
200
210
Stained
Retina
220
Imaging
Software
230
AOTF
240
Digital
Camera
250
Imaging Software
260

Figure 7

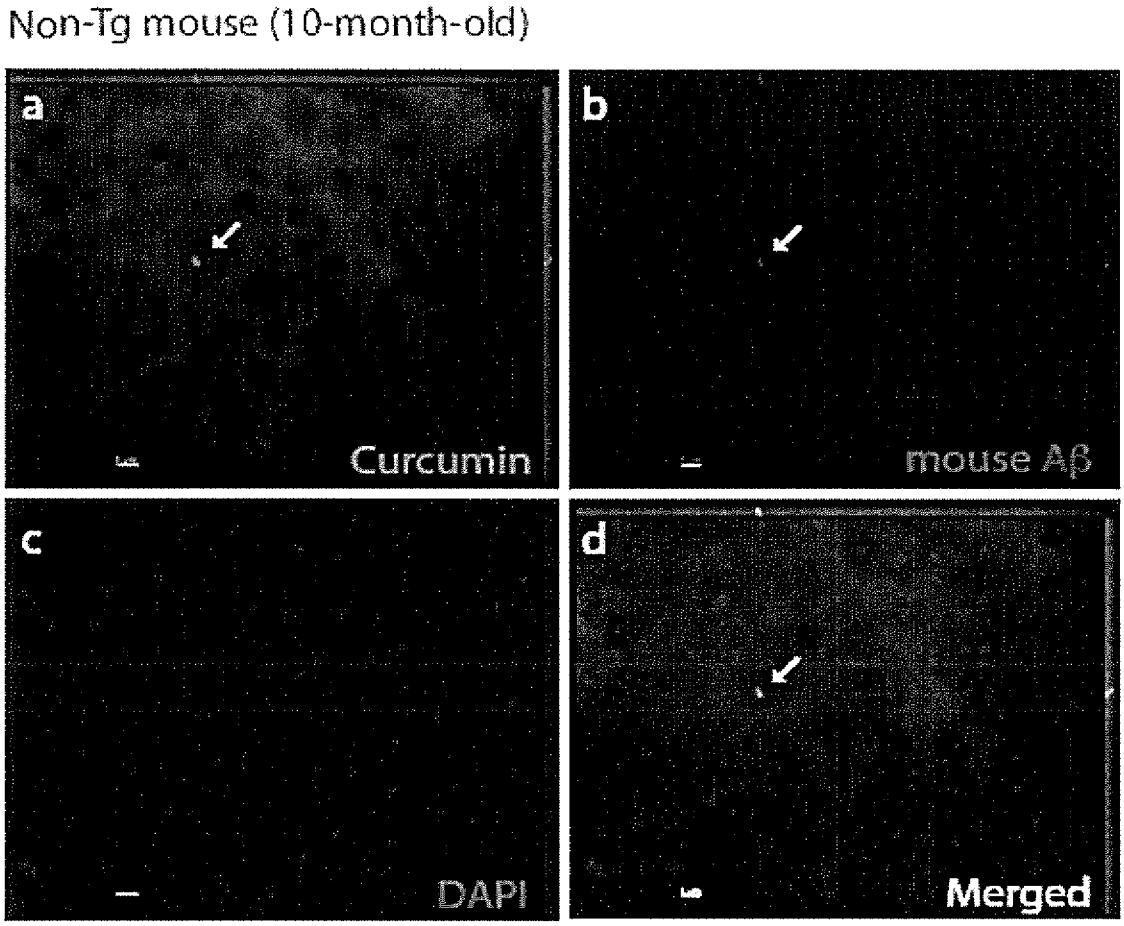

Figure 8

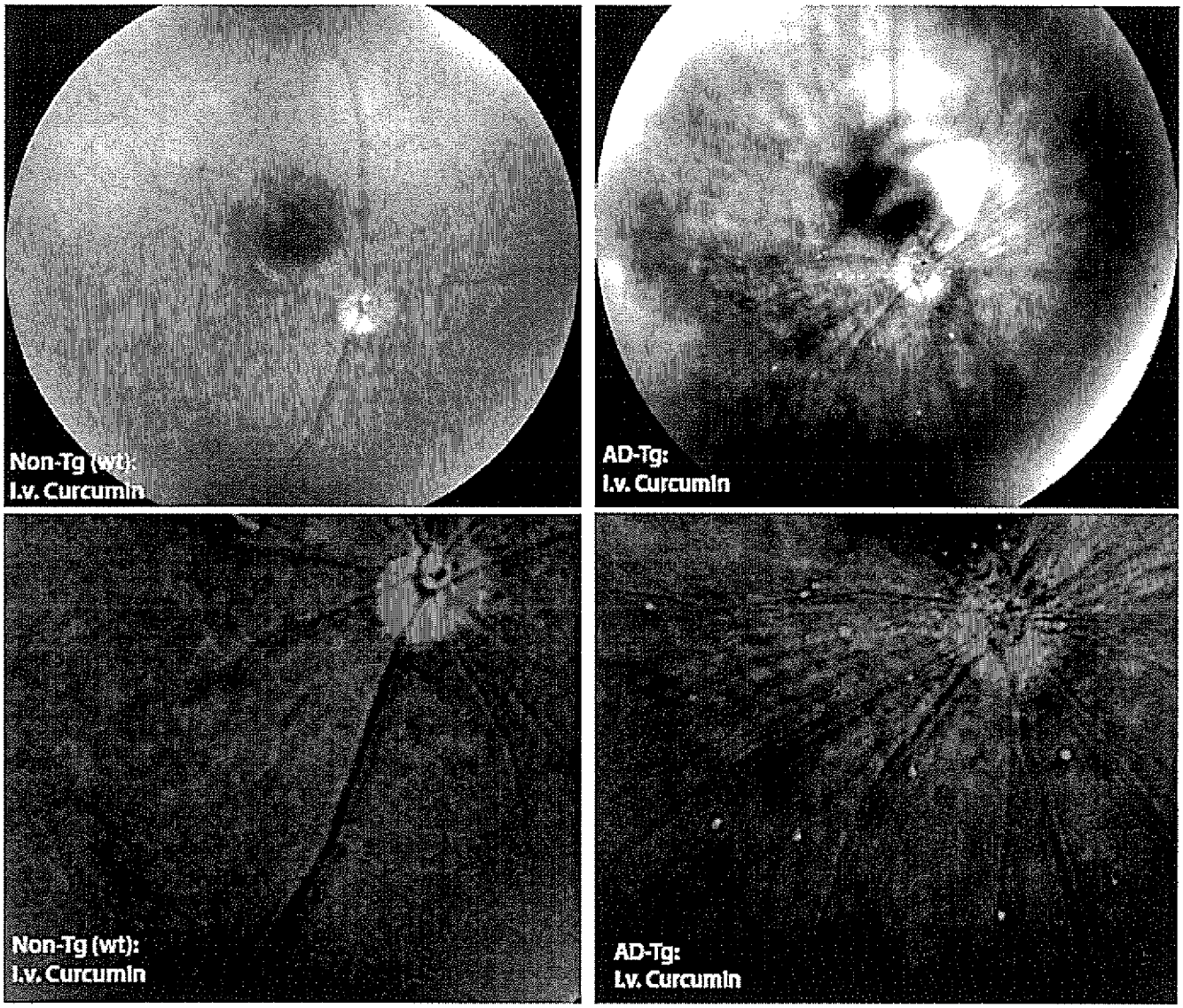
Non-Tg (wt):
I.v. Curcumin
AD-Tg:
I.v. Curcumin
Non-Tg (wt):
I.v. Curcumin
AD-Tg:
I.v. Curcumin

Figure 9

INTERNATIONAL SEARCH REPORT

International application No.
PCT/US 09/57569

A. CLASSIFICATION OF SUBJECT MATTER
IPC(8) - A61K 49/00, C12Q 1/00 (2009.01)
USPC - 435/4, 424/9.6
According to International Patent Classification (IPC) or to both national classification and IPC

B. FIELDS SEARCHED

Minimum documentation searched (classification system followed by classification symbols)
IPC(8) - A61K 49/00, C12Q 1/00 (2009.01)
USPC - 435/4, 424/9.6

Documentation searched other than minimum documentation to the extent that such documents are included in the fields searched
USPC - 435/4, 424/9.6 (keyword delimited)

Electronic data base consulted during the international search (name of data base and, where practicable, search terms used)
PubWEST (PGPB,USPT,USOC,EPAB,JPAB); Google Patents; Google Scholar
Search Terms Used: Alzheimer's, peptides, AB, alpha, beta, ocular, optical, vision, lens, cornea, iris, retina, fluorescent, imaging, spectrometer, curcumin, myelin, derived, agonist

C. DOCUMENTS CONSIDERED TO BE RELEVANT

Category*	Citation of document, with indication, where appropriate, of the relevant passages	Relevant to claim No.
X --- Y	US 2004/0152068 A1 (GOLDSTEIN et al.) 05 August 2004 (05.08.2004), para [0006], [0028], [0029], [0030], [0033], [0039], [0055]	1-3, 6-8, 11-13, 17-19, 23-26 --- 4, 5, 9, 10, 14, 15, 20, 21, 27, 28
X	US 2004/0192588 A1 (EISENBACH-SCHWARTZ et al.) 30 September 2004 (30.09.2004), para [0044], [0045]	16, 22
Y	US 5,987,351 A (CHANCE) 16 November 1999 (16.11.1999), col 1, ln 28-35; col 7, ln 49-56	4, 9, 14, 20, 27
Y	US 2004/0167217 A1 (SCAPAGNINI et al.) 26 August 2004 (26.08.2004), para [0006], [0071]	5, 10, 15, 21, 28

☐ Further documents are listed in the continuation of Box C. ☐

* Special categories of cited documents:
"A" document defining the general state of the art which is not considered to be of particular relevance
"E" earlier application or patent but published on or after the international filing date
"L" document which may throw doubts on priority claim(s) or which is cited to establish the publication date of another citation or other special reason (as specified)
"O" document referring to an oral disclosure, use, exhibition or other means
"P" document published prior to the international filing date but later than the priority date claimed
"T" later document published after the international filing date or priority date and not in conflict with the application but cited to understand the principle or theory underlying the invention
"X" document of particular relevance; the claimed invention cannot be considered novel or cannot be considered to involve an inventive step when the document is taken alone
"Y" document of particular relevance; the claimed invention cannot be considered to involve an inventive step when the document is combined with one or more other such documents, such combination being obvious to a person skilled in the art
"&" document member of the same patent family

Date of the actual completion of the international search	Date of mailing of the international search report
06 November 2009 (06.11.2009)	19 NOV 2009
Name and mailing address of the ISA/US Mail Stop PCT, Attn: ISA/US, Commissioner for Patents P.O. Box 1450, Alexandria, Virginia 22313-1450 Facsimile No. 571-273-3201	Authorized officer: Lee W. Young PCT Helpdesk: 571-272-4300 PCT OSP: 571-272-7774

Form PCT/ISA/210 (second sheet) (April 2007)